Tennessee Valley Authority Kingston Fossil Plant Harriman, Roane County, Tennessee	**Perimeter Containment** **North Dredge Cell (Dike C) Segment 1** **Sta. A161+50 to A179+50**
Document Control Number RDP-0113-E *Calculation Package* FPGKIFFESCDX00030020100006	

Stantec

Exhibit 8
Geophysical Test Results

Purpose:

- Characterize the stiffness of shale bedrock underlying the Kingston Dredge Cell.
- Characterize shallow bedrock conditions.
- Measurements to be used in ground response analyses for predicting severity of earthquake ground motions.

Methods:

- Tests by AECOM:
  - Crosshole Seismic Tests in boreholes
  - Multichannel Analysis of Surface Waves/Microtremor Array Measurements (MASW/MAM) Testing
- Tests by University of Texas at Austin:
  - Spectral Analysis of Surface Waves (SASW) Testing

Results:

- Vertical profiles of shear wave velocities at each test location on the site.
- Results in two separate reports from:
  - AECOM
  - The University of Texas at Austin

Calculation Performed by: AECOM	
Prepared by: C. A. Padar 24-May-09	*Reviewed by:*
Revisions:	
Calculation Performed by: The University of Texas at Austin	
Prepared by: K. H. Stokoe et al. 21-June-10	*Reviewed by:*
Revisions:	

AECOM

Technical Memorandum - Work In Progress

Date: May 4, 2009

To: Bill Walton, Bill Butler

From: Craig A. Padar

Subject: Shear Wave Velocity Testing at TVA Kingston Fossil Plant, Harriman, TN

AECOM Project No. 60095742

Introduction

AECOM is pleased to submit this report detailing the results of shear-wave velocity testing at The Tennessee Valley Authority's (TVA) Ash Pond at Kingston Fossil Plant in Harriman, TN. Seismic shear wave velocity testing was performed at three locations and we were able to measure the shear wave velocity of the ash, alluvium, and the upper shale unit at the site.

Methodology

Crosshole Seismic Testing

The Crosshole Seismic (CHS) surveys were conducted in general accordance with ASTM D-4428/D-4428M. These procedures provide a means of measuring in-situ shear-wave velocity (V_S). AECOM employed an SE&G mechanical, reversible downhole hammer as the *S*-wave acoustic source. Operation of the source consisted of securing the hammer to the source (S) borehole with an inflatable bladder. When the hammer is activated in an up or down direction the energy source produces directionally distorted energy into the surrounding overburden soil and sediments to produce repeatable and identifiable *P*- and *S*-waves. When the source is activated in the opposite direction, the energy produces S-waves with reversed polarity. By stacking multiple hammer strikes on the recording instrument (seismograph), *S*-waves are typically enhanced, whereas other seismic waves and random noise are theoretically out-of-phase and diminished.

Multichannel Analysis of Surface Waves/Microtremor Array Measurements (MASW/MAM) Testing

The combined multichannel analysis of surface waves (MASW) and microtremor array measurement (MAM) in situ shear wave velocity testing was performed at the site by an AECOM geologist/geophysicist. MASW is based on using changes observed in surface wave frequency with increasing distance from the energy source location. For MASW testing, the waves are initiated by a source at the surface (hammer and plate, or acoustic wave generator), and the response is measured by geophones placed at discrete intervals along a specified survey line. AECOM utilized a Geometrics Geode Ultra-light Exploration Seismograph to digitally record seismic field records. A 12 pound sledge hammer was used to initiate seismic waves at both ends of each profile.

Microtremor array measurements as described by Louie (2001) are merged with MASW data section to provide a broader frequency range from which to create shear wave velocity sections. The MAM technique is based on two fundamental principles. The first principle is that common seismic-refraction recording equipment, set out in a way almost identical to shallow P-wave refraction surveys, can effectively record surface waves at frequencies as low as 2 hertz. The second principle is that a simple, two-dimensional slowness-frequency (p-f) transform of a microtremor record can separate Rayleigh waves from other seismic arrivals, and allow recognition of true phase velocity against apparent velocities. Two essential factors that allow exploration equipment to record surface-wave velocity dispersion, with a minimum of field effort, are the use of a single geophone sensor at each channel, rather than a geophone "group array", and the use of a linear spread of 12 or more geophone sensor channels. Single geophones are the most commonly available type, and are typically used for refraction rather than reflection surveying. The advantages of MAM from a seismic surveying point of view are several,

including the following: It requires only standard refraction equipment already owned by most consultants and universities; it requires no triggered source of wave energy; and it will work best in a seismically noisy urban setting. Traffic and other construction vehicles, and possibly the wind responses of trees, buildings, and utility standards provide the surface waves this method analyzes.

Field Design

Inclinometer Cased Holes

The three (3) CHS cased holes at each test location (09-103, 09-211, and 09-301) were installed in a collinear alignment. The acoustic source borehole (S) was selected as one of the end test holes and the far receiver borehole (R2) as the furthest test hole (other end). At the surface, the S borehole was positioned approximately 10 feet from the near receiver borehole (R1) and the R2 borehole was approximately 10 feet beyond R1. Inclinometer measurements were collected in each cased hole at 2-foot depth intervals from 1-to-100 feet below ground surface (bgs), and completed in each of the test holes. Inclinometer-corrected distance measurements will be used to calculate final seismic wave velocities.

Crosshole Seismic Testing

For data collection and recording purposes, GeoStuff™ triaxial downhole geophones with mechanical sidearm were operated in the R1 and R2 receiver boreholes. Geophones were coupled to the inside wall of the receiver boreholes using an electromechanically-operated steel sidearm band. The reversible downhole hammer was lowered down the S borehole and triggered in the same horizontal plane as the receiver (geophone) array. The first test was conducted at 0.5 to 1 feet bgs. The remainder of the digital seismic records was recorded at 5-foot vertical depth increments to 100 feet bgs. Companion tests were also performed for quality control (QC) purposes at 20-foot depth intervals as the source and geophones were extracted from the boreholes. Multiple hammer impacts were stacked for each field record. A Geometrics Geode 24-channel exploration seismograph was utilized to digitally record seismic field records.

Multichannel Analysis of Surface Waves/Microtremor Array Measurements (MASW/MAM) Testing

Two seismic profiles (MASW and MAM) were collected near boreholes 09-103 and 09-211 (where CHS was performed) as well as near 09-208 where surface conditions were favorable for laying out the necessary arrays and where bedrock was thought to be relatively shallow. The first profile (MASW) incorporated a 5-foot geophone spacing and maximum 30-foot source offset to maximize resolution of the 10 to 30 Hz frequency range. The second portion of the data collection (for MAM) at each location involved passively recording background noise using a 20-foot geophone spacing and creating L-shaped profiles that were 100 feet long on each leg to record data in the 2 to 15 Hz range. This L-shaped array is used to reduce any directional bias in the data that might be caused by the location from which the low frequency waves originated.

After collection of seismic field data, the electronic files were transferred to a personal computer for detailed analysis in the office. Wave EQ shear-wave analysis software was used to process the seismic records. The processing for the shear-wave velocities included a Fourier transform of the seismic records, which generates a plot of phase-velocity versus frequency. The dispersion curve can then be identified and an initial velocity model generated. An inversion is then performed to create a velocity model that approximates the observed data.

Data Analysis/Correlation to Boring Logs

Crosshole Seismic Testing

In our opinion, crosshole seismic testing is the most reliable way to get discrete shear-wave interval velocities versus depth through a soil and rock section. The inclinometer-cased holes were installed at boring locations 09-103, 09-211, and 09-301. The first two locations encountered bedrock at 52.5 feet and 53.5 feet respectively. Location 09-301 was installed entirely in unconsolidated fill and native soil material (above bedrock).

At boring location 09-103, shear wave velocity testing was performed on 5-foot depth intervals starting at 1 foot bgs. Table 1 shows the calculated shear wave velocities for the crosshole tests. The unsaturated near-surface material had shear-wave velocities ranging from 844 to 908 feet per second (ft/s). The saturated ash (11, 16, 21-foot depth intervals) shows very slow shear-wave velocities of 425 to 488 ft/s. Then in the 26, 31, and 36-foot depth intervals the velocity appears to increase to 604 to 704 ft/s where the soil description indicates bottom ash. The natural silty clay below the ash at 41 feet bgs showed a shear wave velocity of 757 ft/s. The 46-foot depth interval (in sandy silt) showed a velocity of 498 ft/s. Overall the shear wave velocity increased from 425 to 757 ft/s through overburden materials which had Standard Penetration Test (SPT) blowcounts (N-values) ranging from 1 to weight-of-hammer (WOH), and weight-of-rods (WOR) for 1 foot or more penetration. No shear waves were observed in bedrock for seismic records below 46 feet. See the paragraph at the end of this section for a discussion of this observed condition. The piezo-cone penetrometer testing (CPT_u) performed at this location agrees well with the descriptions and SPT N-values for the materials observed.

At boring location 09-211, CHS data was collected through an undisturbed section of Dike C fill material, emplaced ash and underlying natural sediments. The shear wave velocity of the upper clay fill (dike material) varied from 1,988 ft/s in the highly compacted surface material, to 922 to 1,076 ft/s down to 15 feet bgs. Shear wave velocities varied from 815 to 1,334 ft/s in the bottom ash noted from 15.3 to 24 feet bgs. A sandy clay layer was observed in SPT boring 09-211 from 25 to 28 feet and CHS testing in this interval calculated a shear wave velocity of 1,334 ft/s. Clayey silt and silty sand was noted in the 09-211 boring log from 28 to 37.5 feet bgs and the calculated shear wave velocities were 834 to 856 ft/s respectively. Well graded sands were observed from 37.5 to 53.5 feet bgs and the shear wave velocity varied from 654 to 729 ft/s. This decrease in shear wave velocity corresponds with the zone from 32 to 48 feet bgs where SPT N-values ranged from WOH for 1.0 foot to one hammer blow for 2.5 feet (N-value < 1). The CPT_u performed at this location shows tip resistances that correspond well with the SPT N-values and material classifications on the boring log for this boring. Similar to the CHS test performed at 09-103, no shear waves were able to be measured below the bedrock interface at 53.5 feet and this issue is further discussion at the end of this section.

At boring location 09-301, CHS test was performed from the top of the remaining intact Cell No. 1 ash pile. The cased holes are entirely in unconsolidated materials (unfailed ash). The shear wave velocities vary from 450 to 651 ft/s from 0 to 50 feet in the sluiced fly ash. Low SPT N-values through the unfailed ash correspond well with the low shear wave velocities. A zone of harder materials described as bottom ash correlates with an increase in shear wave velocity (850 to 877 ft/s) from 50 to 60 feet. Deeper portions of fly ash show velocities of 672 to 911 ft/s. Softer natural clays below 90 feet bgs showed shear wave velocities of 619 to 718 ft/s.

It is possible that conditions exist in the bedrock that have caused borehole sidewall softening or a layer of water content or smeared drill cuttings formed around the grout placed within the annular space adjacent to the inclinometer casing. If the material around the well casing is fluid-like, there can be no transmission of the shear wave through fluid. In an attempt to gather data at intervals which may still contain competent grout below the bedrock surface, the CHS array was collected with the source at either end of the well array as well as shot from the middle inclinometer casing. Further, testing was performed at 2.5 ft intervals below the elevation where shear wave loss was observed in case some zones of grout remained intact. No shear waves were measured or detected during additional testing. The compression wave (p-wave) is still visible so equipment malfunction was ruled out. Additional troubleshooting included shifting the recording time to start before the trigger in case a timing issue existed. Analysis of these records determined that there was no “missing” signal before time zero.

Multichannel Analysis of Surface Waves/Microtremor Array Measurements (MASW/MAM) Testing

The results of the MASW/MAM surveys are tabulated as layer velocities and are shown on Table 2. The shear wave velocities range from 364 feet per second (fps) in loose near-surface materials to 1,787 ft/s near a depth of 100 feet below grade. The 100-foot average shear wave velocity over profiles at 09-301, 09-211, and 09-208 is 853, 1,214, and 1,095 ft/s respectively. The calculated 100-foot average for

09-211 may be slightly higher than it actually is due to space considerations near the borehole. The arrays were collected in a straight-line configuration only because there was not enough space to lay out an L-shaped array for the MAM. Wave fronts that encounter the array at a high angle appear to pass through the array faster than waves that originate off the ends of the array.

The modeled section created for 09-103 boring location shows shear wave velocities that correlate with the materials described in the boring log. A low modeled velocity is shown from 8 to 11 feet bgs where very loose saturated ash material was noted on boring log. The modeled velocity is 145 ft/s and is probably lower than the actual shear wave velocity. Shear wave velocities modeled for the fly ash vary from 360 to 633 ft/s with the majority of the velocities falling in the 500 to 550 ft/s range. The average velocity in the natural silts and clays increases slightly and varies from 666 to 854 ft/s. Bedrock shale velocities vary from 1,019 to 1,325 ft/s

The tested MASW/MAM section for 09-211 boring location also shows good correlation between model velocities and the described material and standard penetration resistance numbers. The clayey dike material velocities vary from 650 to 833 ft/s in the upper 12 feet. A hard zone of bottom ash was noted from 15 to 20 ft and is seen on the velocity model as a 900 to 950 ft/s layer. Extremely soft and/or loose materials having SPT N-values of WOH or N-values less than 8 blows per foot consisting of thin layer of fly ash then natural clays and sands. The modeled velocities for these layers vary from 512 to 672 ft/s. The bottom 10 feet of the natural sands show shear wave velocities of 972 ft/s, although the material still has very low SPT N-values. Computed shale bedrock velocities increase quickly with depth from 1,199 to 1,787 ft/s

An additional MASW/MAM survey was conducted near the boring location of 09-208 to obtain more shale bedrock velocities. This location has enough relatively flat ground to collect the MASW and the MAM L-shaped array. The ground surface elevation for the seismic array was about 5 feet higher than the borehole location and the elevations shown on Table 2 have been adjusted accordingly. The velocity of the fly ash in the upper 6 feet varied from 255 to 348 ft/s in the model. The natural clayey sand and sand velocities vary from 424 to 777 ft/s and show an increase in velocity with depth. The velocity increases gradually into the bedrock and varies from 883 ft/s near the bedrock interface to 1,410 ft/s at 92 feet bgs.

The MASW/MAM methods are not a direct measurement of the s-wave (i.e., shear wave) at discrete depth intervals, but rather an average across the length of the seismic array. Therefore, modeled sections are expected to vary from direct interval measurements as would be performed in CHS surveys.

Summary

The following points summarize the findings of the surveys performed to determine shear wave velocities as described above.

- CHS testing was performed in inclinometer-cased holes at 3 locations within the dredge cell area.
- No shear waves from the CHS tests were observable below the top of the bedrock surface due to problems in the casing/grout interface with the drilled shale.
- The testing program was supplemented by MASW/MAM surface wave methods to obtain shale bedrock shear wave velocity information.
- Velocity ranges observed for the various materials at the site are as follows:
    - Clayey dike material - 650 to 900 ft/s;
    - Loose surface materials and fly ash - 250 to 680 ft/s; bottom ash 780 to 1,035 ft/s;
    - Natural clays below ash - 420 to 800 ft/s;
    - Natural sands above shale bedrock - 700 to 950ft/s;
    - Fractured shale bedrock - 883 to 1,787ft/s.
- In general, there is a strong correlation between the CPT_u resistances across the site. The shear wave velocities also correlate well with variations shown on the boring log (i.e., material descriptions). The SPT N-values show a general conformance to shear wave variations in the section but still vary considerably when in materials has SPT readings of WOH or WOR.

- The MASW/MAM testing performed at 09-211 shows shear wave velocities that are 25 to 35 percent higher than the tests performed at 09-301 and 09-208. This may be a directional bias in the deeper values caused by using a MAM array that had to be laid out in a straight line and not an "L" shaped array due to space considerations next to wet ash.
- The MASW/MAM modeled average velocities through a large zone of material and as a result are less precise than CHS testing at discrete depth intervals. The CHS should be relied upon for shear wave velocities above bedrock and MASW/MAM data used to shear wave velocities in shale bedrock.

See the attached tables and figures that summarize the collected data versus depth and test method. There is some data scatter due to failed and unfailed ash and geologic variability.

References

ASTM Standard D4428 / D4428M - 07 "Standard Test Methods for Crosshole Seismic Testing", ASTM International, West Conshohocken, PA, www.astm.org

Louie, J, N., 2001, Faster, Better: Shear-wave velocity to 100 meters depth from refraction microtremor arrays: Bulletin of the Seismological Society of America, v. 91, p. 347-364.

Park, C.B., Miller, R.D., and Xia, J., 1999, Multichannel analysis of surface waves (MASW); Geophysics, 64, 800-808. [PDF available online, 1.3 MB]

Attachments:

Figure 1: Shear Wave Velocities from CHS and MASW/MAM
Table 1: Shear Wave Velocities Determined by Crosshole Seismic Testing
Table 2: Shear Wave Velocities Determined by MASW/MAM Surveys

FIGURE 1. Shear Wave Velocities from CHS and MASW/MAM

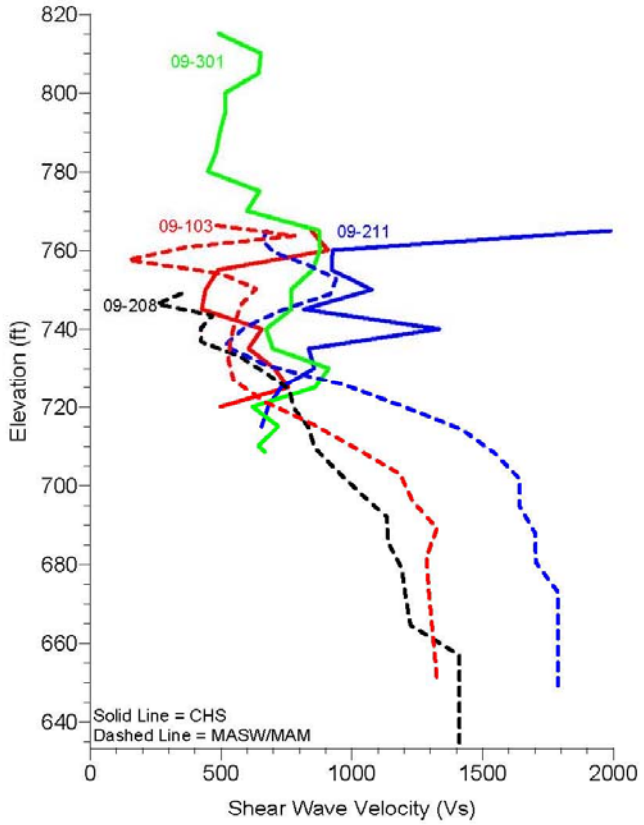

TABLE 1. Shear Wave Velocities Determined by Crosshole Seismic Testing.

09-103			09-211			09-301		
Depth	Elevation	Velocity ft/s	Depth	Elevation	Velocity ft/s	Depth	Elevation	Velocity ft/s
1	765	844	0.5	765	1988	1	815	491
6	760	908	5.5	760	926	6	810	651
11	755	488	10.5	755	922	11	805	643
16	750	440	15.5	750	1076	16	800	516
21	745	425	20.5	745	815	21	795	516
26	740	656	25.5	740	1334	26	790	495
31	735	604	30.5	735	834	31	785	481
36	730	704	35.5	730	856	36	780	450
41	725	757	40.5	725	729	41	775	647
46	720	498	45.5	720	679	46	770	599
51	715	**	50.5	715	654	51	765	875
56	710	**	55.5	710	**	56	760	877
61	705	**	60.5	705	**	61	755	850
66	700	**	65.5	700	**	66	750	767
71	695	**	70.5	695	**	71	745	767
76	690	**	75.5	690	**	76	740	672
81	685	**	80.5	685	**	81	735	697
86	680	**	85.5	680	**	86	730	911
91	675	**	90.5	675	**	91	725	859
96	670	**	95.5	670	**	96	720	619
101	665	**	100.5	665	**	101	715	718
						106	710	642
						107.5	708.5	668
						Average Shear Wave Velocity Over 100ft Interval (Vs100) ft/s		671.5

** Denotes zone where shear-wave was not observed in the seismic record. Records were further collected in between each interval where the shear wave was not observed in the bedrock portion of the holes.

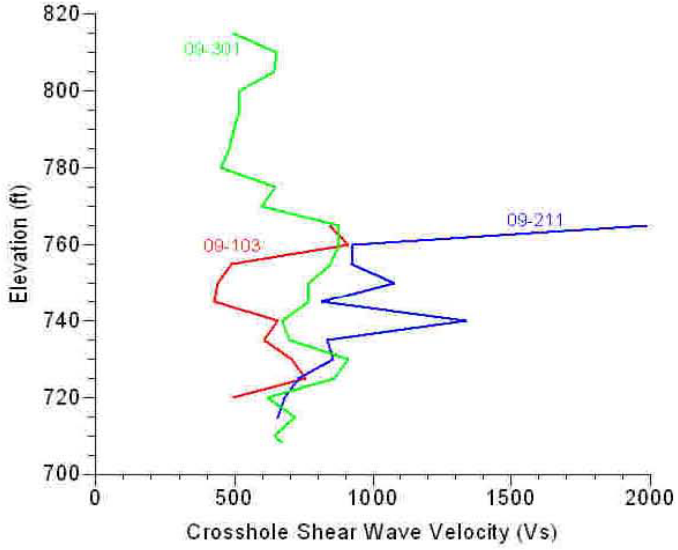

TABLE 2. Shear-Wave Velocities Determined by MASW/MAM Surveys

09-103			09-211			09-208		
Depth(ft)	Elevation	S-velocity(ft/s)	Depth(ft)	Elevation	S-velocity(ft/s)	Depth(ft)	Elevation	S-velocity(ft/s)
0.0	766.3	483	0.0	765.0	673	0.0	749.0	348
2.6	763.7	781	2.6	762.4	659	2.6	746.4	255
5.6	760.8	364	5.6	759.4	703	5.6	743.4	467
8.8	757.5	145	8.8	756.2	833	8.8	740.2	423
12.3	754.0	501	12.3	752.7	940	12.3	736.7	424
16.1	750.2	633	16.1	748.9	917	16.1	732.9	573
20.2	746.1	575	20.2	744.8	733	20.2	728.8	671
24.6	741.7	553	24.6	740.4	590	24.6	724.4	761
29.2	737.1	535	29.2	735.8	512	29.2	719.8	777
34.2	732.1	528	34.2	730.8	672	34.2	714.8	833
39.5	726.8	548	39.5	725.5	974	39.5	709.5	858
45.0	721.3	666	45.0	720.0	1199	45.0	704.0	939
50.9	715.4	854	50.9	714.1	1423	50.9	698.1	1030
57.0	709.3	1019	57.0	708.0	1550	57.0	692.0	1134
63.5	702.9	1184	63.5	701.5	1642	63.5	685.5	1138
70.2	696.1	1231	70.2	694.8	1640	70.2	678.8	1191
77.2	689.1	1325	77.2	687.8	1700	77.2	671.8	1205
84.5	681.8	1285	84.5	680.5	1703	84.5	664.5	1224
92.1	674.2	1292	92.1	672.9	1787	92.1	656.9	1410
115.8	650.5	1325	115.8	649.2	1787	115.8	633.2	1410
Average Shear Wave Velocity to 100 ft (Vs100)		853 ft/s	Average Shear Wave Velocity to 100 ft (Vs100)		1214 ft/s	Average Shear Wave Velocity to 100 ft (Vs100)		925 ft/s

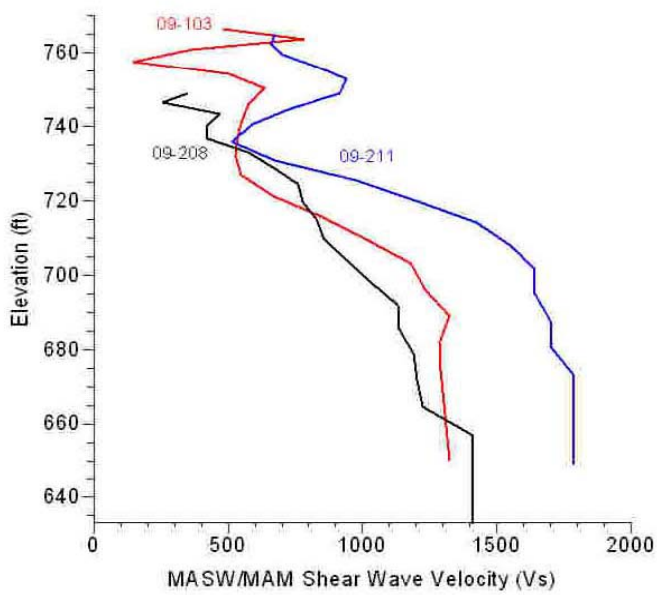

FIELD DATA REPORT (FDR): SASW TESTING AT KINGSTON FLY ASH RECOVERY PROJECT, HARRIMAN, TENNESSE

for

Stantec Consulting Services
100 Westwood Place, Suite 420
Brentwood, TN 37027

by

Kenneth H. Stokoe, II
Jiabei Yuan
Changyoung Kim

June 21, 2010

Geotechnical Engineering Report GR10-02
Geotechnical Engineering Center
Civil Engineering Department
The University of Texas at Austin

TABLE OF CONTENTS

TABLE OF CONTENTS i
LIST OF TABLES ii
LIST OF FIGURES iii
1. Introduction 1
2. Overview of the SASW Test Method 3
3. Summary of Field Testing and Analysis Procedures 9
3.1 Field Equipment and Testing Procedures 9
3.2 Spectral Calculations 14
3.3 Data Reduction and Forward Modeling Procedure 16
3.3.1 Constructing Individual and Composite Field Dispersion Curves 17
3.3.2 Matching the Composite Field and Theoretical Dispersion Curves 20
3.3.3 Additional Considerations 20
4. Discussion of the V_s Profiles 24
5. Summary and Conclusions 27
6. References 28
Appendix A – Parameters Used to Obtain the V_s Profile of Each SASW Test Site at the Kingston Fly Ash Recovery Project, Harriman, TN A-1
Appendix B - Individual V_s Profiles of the 9 SASW Test Sites at the Kingston Fly Ash Recovery Project, Harriman, TN B-1
Appendix C - Interpreted V_s Profiles of the 9 SASW Test Sites at the Kingston Fly Ash Recovery Project, Harriman, TN C-1

LIST OF TABLES*

Table 1 Coordinates, Elevations and Estimated Water Tables of Nine SASW Sites 9

Table 2 Typical Source-Receiver Spacings Used in SASW at the Kingston Fly Ash Recovery Site 10

Table 3 Parameters Used to Obtain the V_S Profile at SASW Site No. 5, Kingston Fly Ash Recovery Project, Harriman, TN 21

*Note – Tables in Appendix A are not listed.

LIST OF FIGURES*

Figure 1 Locations of Nine SASW Sites Tested at the Kingston Fly Ash Recovery Site 2

Figure 2 Illustration of Surface Waves with Different Wavelengths Sampling Different Materials in a Layered System 4

Figure 3 Schematic Diagram of the Generalized Equipment Arrangement Used in Spectral-Analysis-of-Surface-Waves (SASW) Testing for One Receiver Pair 4

Figure 4 Comparison of Shear Wave Velocity Profiles from SASW and Crosshole Measurements Performed at a Site on Treasure Island near San Francisco, CA (Joh, 1996; Fuhriman and Stokoe, 1993) 6

Figure 5 Comparison between SASW and Downhole V_S profiles at Site H2 in Hanford, WA (Stokoe et al., 2005) 7

Figure 6 Comparison of SASW and Downhole Median Profiles of Both Sand and Gravel Sequences in the Hanford Formation (Stokoe et al., 2005) 8

Figure 7 Common-Middle-Receiver Geometry Used in SASW Testing at the Kingston Fly Ash Recovery Project Site 10

Figure 8 Photograph of Liquidator (from http://nees.utexas.edu/Home.shtml) 12

Figure 9 Photograph of 1-Hz Geophone Semi-Embedded in the Ground and the Pre-Test Check for Plumbness (Illustrative Photograph taken at Hanford, WA) 12

Figure 10 Photograph of Three, 1-Hz Geophones at One Receiver Set-up; SASW Site Site No. 2 at the Kingston Fly Ash Recovery Project 13

Figure 11 Photograph of Personnel Using the Sledge Hammer Source at Hanford, WA 13

Figure 12 Photograph of Liquidator Working at SASW Site No. 5 of the Kingston Fly Ash Recovery Project 15

*Note – Figures in Appendices B through C are not listed.

LIST OF FIGURES* (CONTINUED)

Figure 13 Wrapped Phase of the Transfer Function Measured at SASW Site No. 5 with Liquidator as the Seismic Source and a 50-ft, S-R#1 Receiver Spacing 18

Figure 14 Individual Experimental Dispersion Curve Created from the Unwrapped Phase Record in Figure 12b Measured with a 50-ft Receiver Spacing (50 ft between the Receiver Pair) at SASW Site No. 5 19

Figure 15 Composite Experimental Dispersion Curve Created from Phase Measurements Performed at all Receiver Spacings at SASW Site No. 5 using the Sledge Hammer and Liquidator as the Seismic Sources 19

Figure 16 Comparison of the Fit of the Theoretical Dispersion Curve to the Composite Experimental Dispersion Curve at SASW Site No. 5 21

Figure 17 Final Shear Wave Velocity Profile Determined at SASW Site No. 5 22

Figure 18 Statistic Analyses of V_s Profiles of the Unweathered Shale Identified in the Interpreted Profiles in Appendix C 26

*Note – Figures in Appendices B through C are not listed.

FIELD DATA REPORT

1. Introduction

This report presents the findings from Spectral-Analysis-of-Surface-Waves (SASW) tests that were performed at nine locations as part of the geotechnical engineering investigation for the Kingston Fly Ash Recovery Project at Harriman, TN. Field testing was performed during April 27 through 30, 2010 using a large vibroseis called "Liquidator" as the high-energy source following the generalized procedure described in Stokoe et al., 1994. The locations of the nine SASW sites are shown in Figure 1. Professor Kenneth H. Stokoe, II, Mr. Jiabei Yuan, Mr. Changyoung Kim and Mr.Curtis E. Mullins from the University of Texas at Austin (UT) performed the SASW tests in the field. Analysis of the SASW data to develop shear wave velocity profiles (V_s) was performed by Mr. Jiabei Yuan and Professor Stokoe at UT.

The goal of the seismic investigation was to characterize the shear wave velocity (V_s) of the soil/fly ash/rock profiles at the Kingston site. This goal was accomplished by: (1) developing V_s profiles to depths ranging from 192 to 405 feet at the nine sites, and (2) comparing the V_s profiles from the different test locations to investigate the stiffnesses of the geologic materials, the variability in the material stiffnesses, and the estimated depth to bedrock.

The field data report documenting the SASW testing is presented herein. The report contains a discussion of the SASW test method as applied at the Kingston Project. The SASW field test and data analysis procedures are described. An example of the measurements performed at one SASW site is presented. The V_s profiles determined at all nine sites are then discussed. Each V_s profile is presented individually in Appendix A in tabular form and in Appendix B in graphical form. An interpretation of the material profile at each site is also briefly discussed. The interpreted profiles are presented in Appendix C.

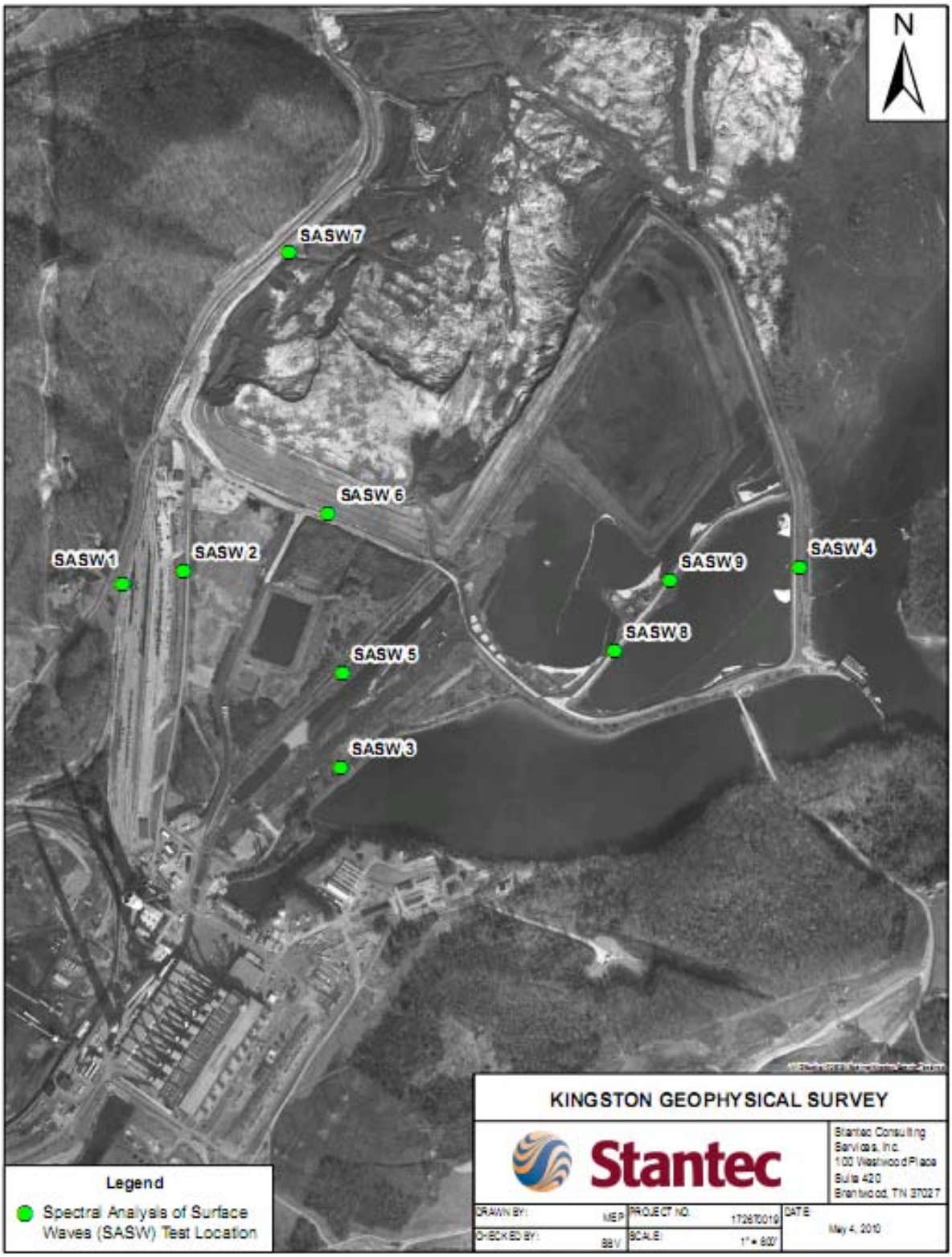

Figure 1 Locations of Nine SASW Sites Tested at the Kingston Fly Ash Recovery Site

2. Overview of the SASW Test Method

The SASW test method is a nondestructive and nonintrusive seismic method. The method utilizes the dispersive nature of Rayleigh-type surface waves propagating through a layered material to determine the shear wave velocity profile of the material (Stokoe et al., 1994). In this context, dispersion arises when surface wave velocity varies with wavelength or frequency. Dispersion in surface wave velocity arises from changing stiffness properties of the soil and rock layers with depth. This phenomenon is illustrated in Figure 2 for a multi-layered solid. A high-frequency surface wave, which propagates with a short wavelength, only stresses material near the exposed surface and thus only samples the properties of the shallow, near-surface material (Figure 2b). A lower-frequency surface wave, which has a longer wavelength, stresses material to a greater depth and thus samples the properties of the shallower and deeper materials (Figure 2c). Spectral analysis is used to separate the waves by frequency and wavelength to determine the experimental ("field") dispersion curve for the site. An analytical, forward - modeling procedure is then used to theoretically match the field dispersion curve with a one-dimensional layered system of varying layer stiffnesses and thicknesses (Joh, 1996). The one-dimensional shear wave velocity profile that generates a dispersion curve that most closely matches the field dispersion curve is presented as the shear wave velocity profile at the site.

SASW testing involves generating surface waves at one point on the exposed material surface and measuring the motions perpendicular to the surface created by the passage of surface waves at two or more locations on the surface. All measurement points are arranged on the exposed surface along a single radial path from the source. Successively longer spacings between the receivers and between the source and first receiver are typically used to measure progressively longer and longer wavelengths. This general testing configuration for one source/receiver set-up is illustrated in Figure 3. In this example, a source and two receivers are used. The distance between the source and first receiver (d) is kept equal to the distance between the two receivers (d) as shown in Figure 3. Testing is performed with several (typically six or more) sets of source-receiver spacings, and the totality of the sets of source-receiver spacings is called an SASW array.

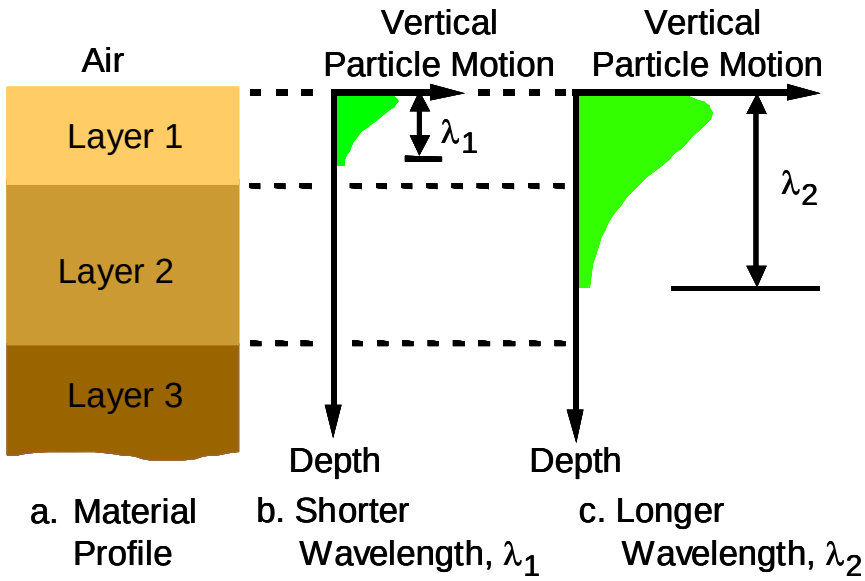

Figure 2 Illustration of Surface Waves with Different Wavelengths Sampling Different Materials in a Layered System

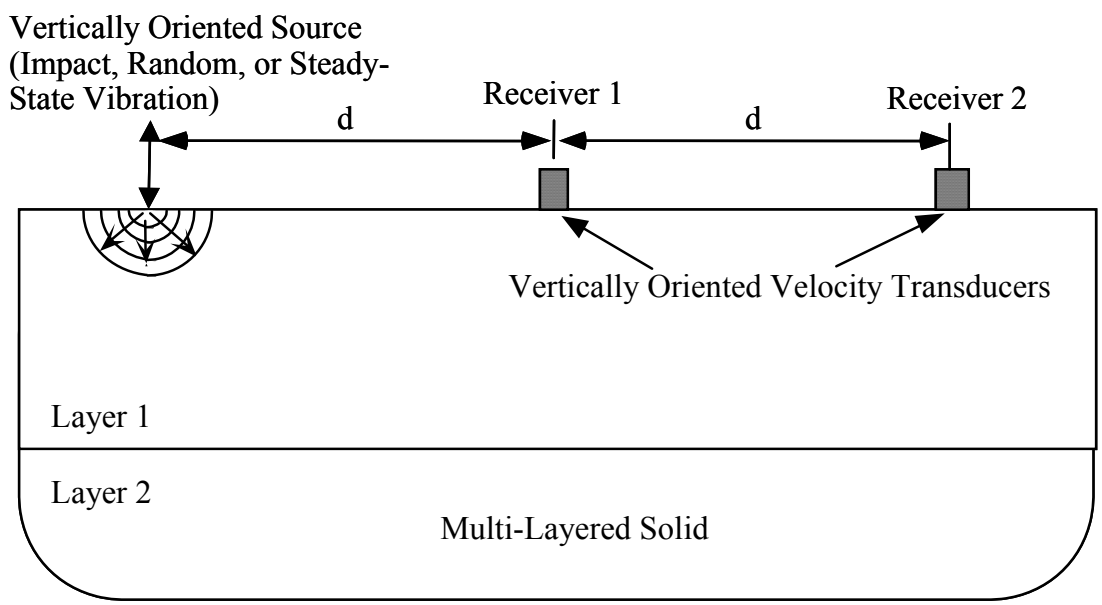

Figure 3 Schematic Diagram of the Generalized Equipment Arrangement Used in Spectral-Analysis-of-Surface-Waves (SASW) Testing for One Receiver Pair

The variation in phase shift with frequency for surface waves propagating between adjacent receivers is recorded for each receiver spacing. From each receiver pair, the phase velocity of the surface wave can be calculated at each frequency from:

$$V_R = f \bullet \frac{360}{\phi} \bullet d \tag{1}$$

where V_R is the phase velocity in ft / sec or m/s, f is the frequency in Hertz (cycles per sec), ϕ is the phase angle in degrees (at frequency f), and d is the distance between the receivers in the same length units as used to represent V_R. From this calculation, a plot of phase velocity versus frequency, called an individual dispersion curve, is generated. This procedure is repeated for all source-receiver spacings used at the site and typically involves significant overlapping in the dispersion data between adjacent receiver sets. The individual dispersion curves from all receiver spacings are combined into a single composite dispersion curve called the "experimental" or "field" dispersion curve.

Once the composite field dispersion curve is generated for the site, an iterative forward modeling procedure is used to create a theoretical dispersion curve to match the experimental curve (Joh, 1996). The stiffness profile that provides the best match to the experimental dispersion curve is presented as the shear wave velocity, V_s, profile at the site. Typical comparisons between V_s profiles measured by SASW testing and by independent crosshole and downhole seismic tests are presented in Figures 4, 5 and 6 for work conducted in earlier studies (Joh, 1996; Fuhriman and Stokoe, 1993; Stokoe et al, 2005).

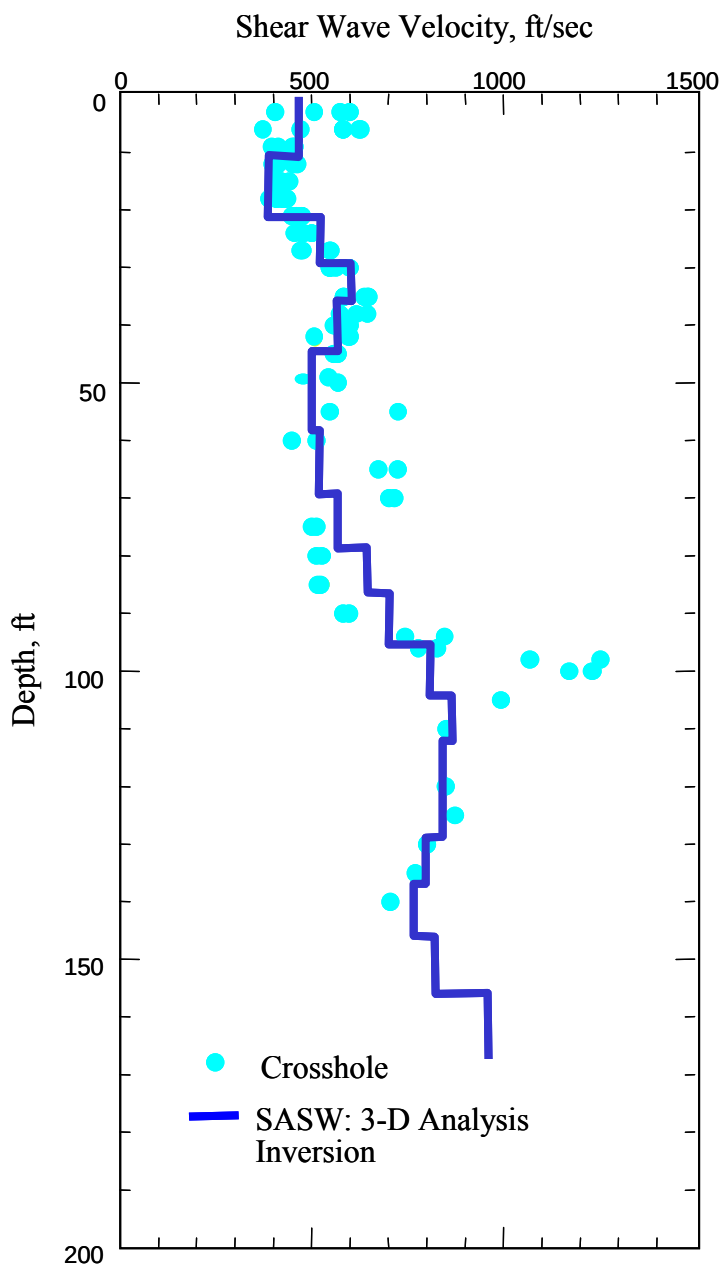

Figure 4 Comparison of Shear Wave Velocity Profiles from SASW and Crosshole Measurements Performed at a Site on Treasure Island near San Francisco, CA (Joh, 1996; Fuhriman and Stokoe, 1993)

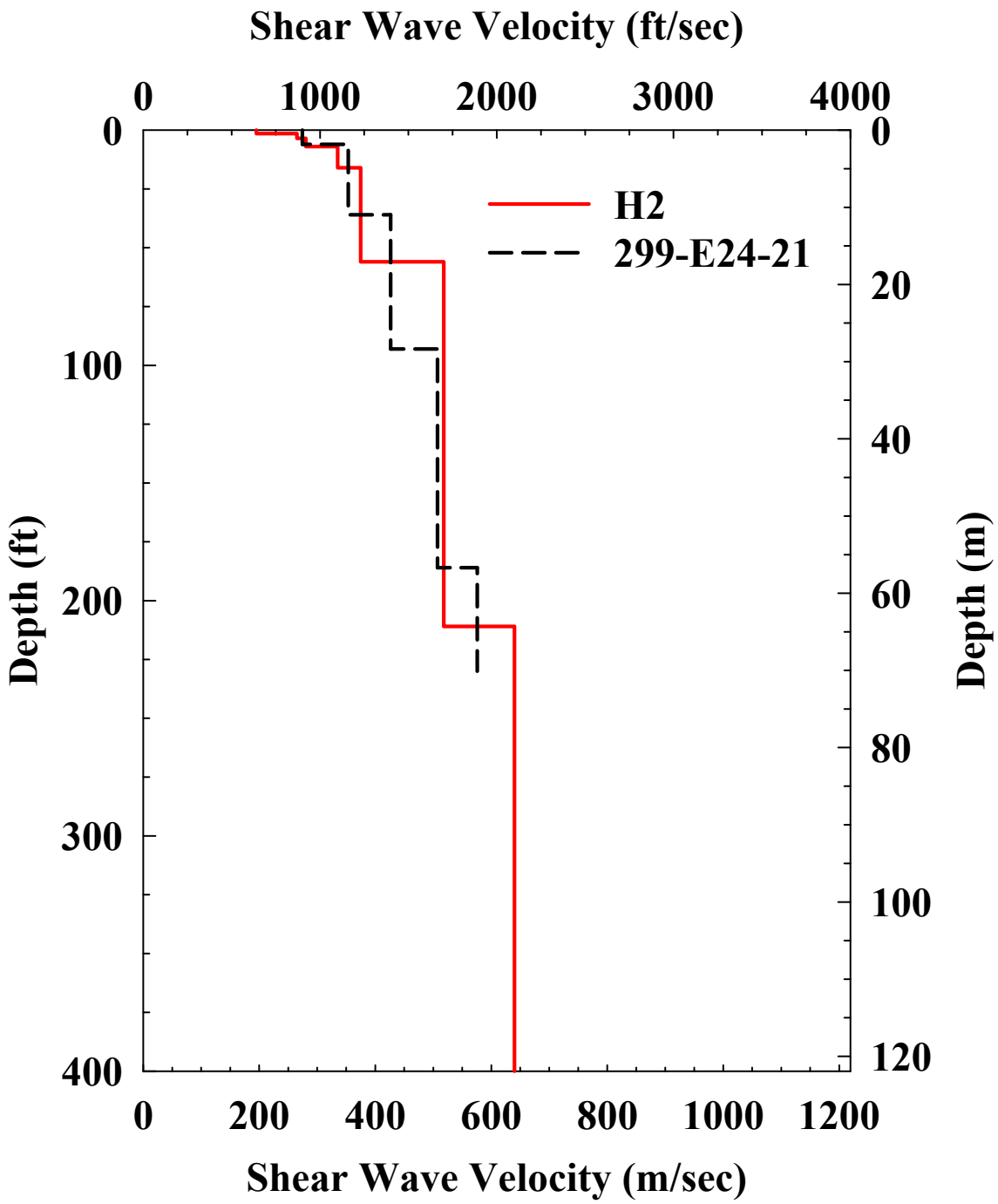

Figure 5 Comparison between SASW and Downhole V_S profiles at Site H2 in Hanford, WA (Stokoe et al., 2005)

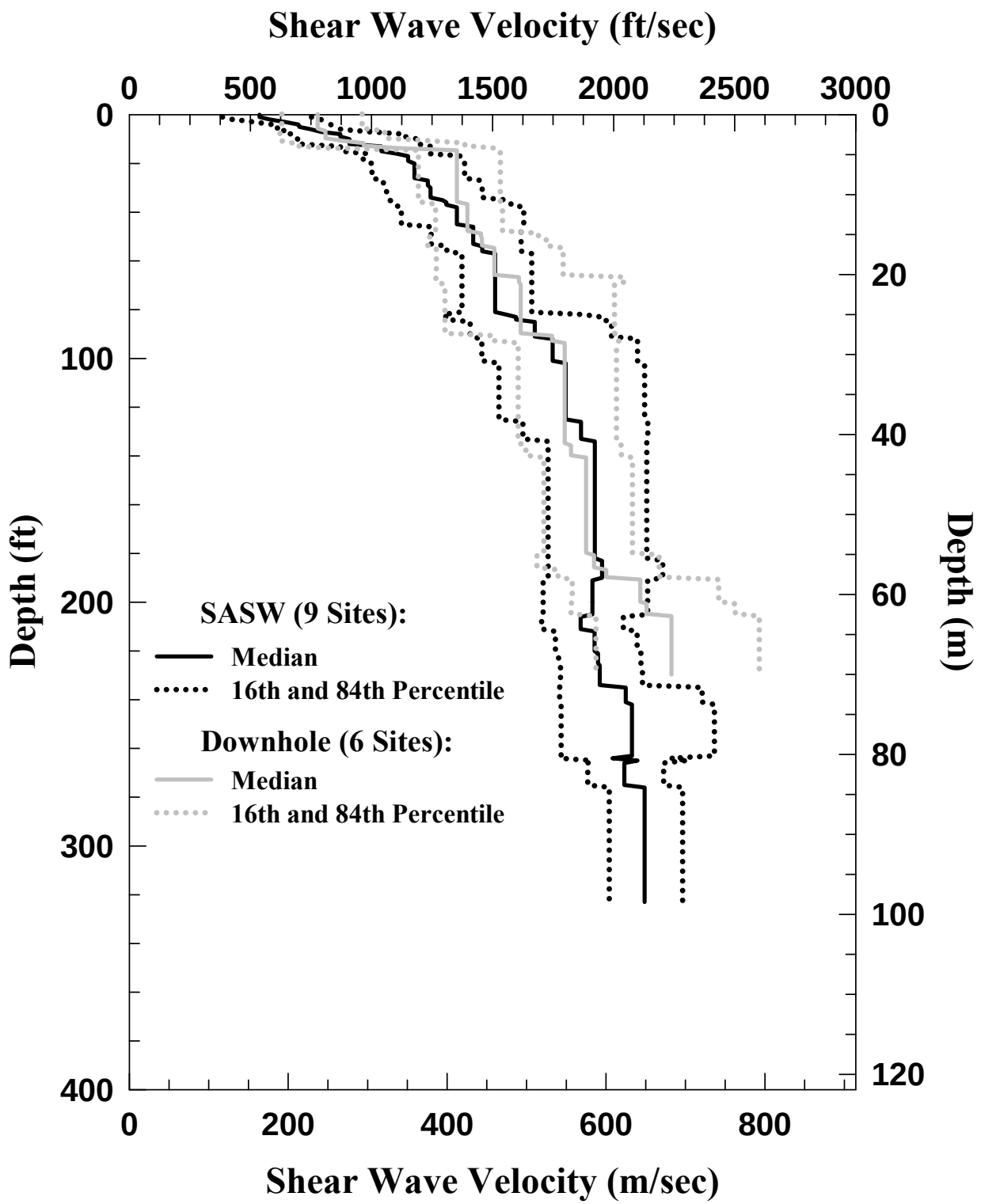

Figure 6 Comparison of SASW and Downhole Median Profiles of Both Sand and Gravel Sequences in the Hanford Formation (Stokoe et al., 2005)

3. Summary of Field Testing and Analysis Procedures

3.1 Field Equipment and Testing Procedures

A total of nine SASW test sites were evaluated at locations around the Kingston Fly Ash Recovery Site. The ground elevations and estimated water table depths at the center points of the nine sites are given in Table 1. The seismic source used for the larger source-receiver spacings during this effort was Liquidator as discussed below.

Table 1 Coordinates, Elevations and Estimated Water Table Depths at the Nine SASW Sites

Survey No. *	Northing (ft)	Easting (ft)	Elevation (ft)	Site No.	Water Table Depth* (ft)
1000	554580.9	2442020	765.646	SASW 9	18
1001	554107.6	2441644	765.917	SASW 8	18
1002	553958.1	2439804	768.662	SASW 5	21
1003	555033.5	2439711	767.633	SASW 6	20
1004	556792.1	2439443	765.313	SASW 7	18
1005	553325.9	2439790	754.123	SASW 3	14
1006	554561.5	2438323	769.909	SASW 1	22
1007	554648.9	2438730	764.275	SASW 2	17
1008	554675.5	2442892	750.76	SASW 4	11

* Surveys and estimated depth to water table given by Stantec Consulting Services.

The basic configuration of the source and receivers used in field testing at each array location is illustrated in Figure 7. Three receivers were used at each source/receiver set-up. This arrangement enabled two sets of SASW test results (two individual dispersion curves as discussed below) to be obtained at the same time, thereby cutting testing time in half as compared to using only two receivers (as illustrated in Figure 3). The middle receiver (Receiver #2) was located at the center line of the test array at all times. When different spacings were used and/or reverse directions were tested, only Receivers #1 and #3 and the source were moved. For the shorter spacings, usually source-to-receiver spacings of 3, 6, 12 and 25 ft, tests were performed in both the forward and reverse directions using a sledge hammer for an impact source. In some cases, the sledge-hammer source was also used at spacings of 40 and 80 ft. For the larger spacings, often beginning at source-to-receiver spacings of 50 ft, testing was performed only in the forward direction using a large vibroseis, called “Liquidator”, as the source. Figure 8 is a photograph of Liquidator from the Nees@UTexas website. Reverse direction testing was typically not performed with liquidator due to the limited testing space.

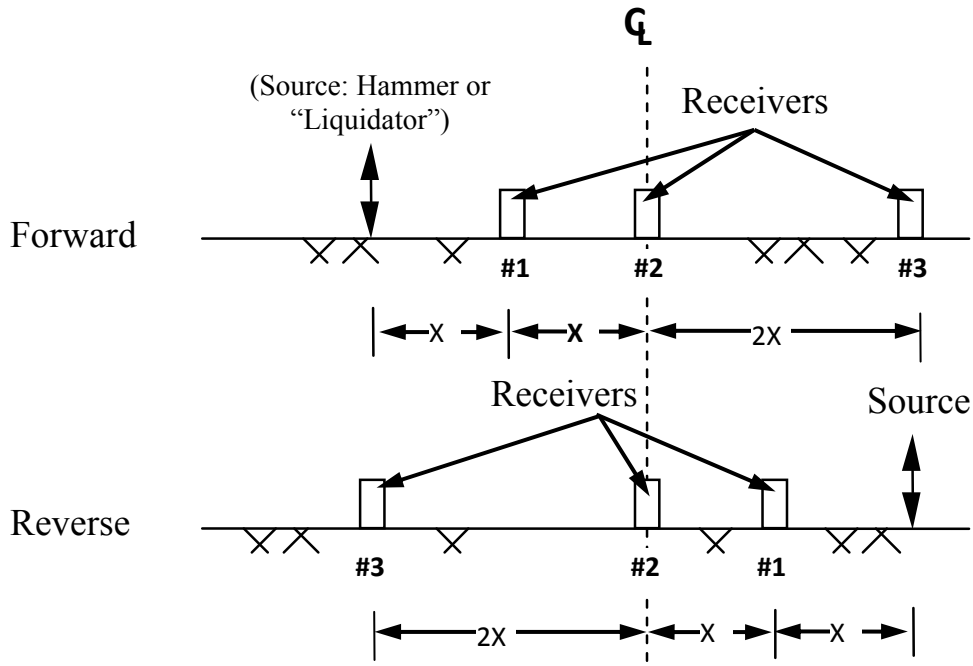

Figure 7 Common-Middle-Receiver Geometry Used in SASW Testing at the Kingston Fly Ash Recovery Project Site

Table 2 Typical Source-Receiver Spacings Used in SASW at the Kingston Fly Ash Recovery Site

Distance			Impact Direction		Source	Frequency (Hz) Range	No. of Pts.	Window
S-R1*	**R1-R2#**	**R2-R3Δ**	**Forward**	**Reverse**				
3	3	6	√		Hammer	0 - 400	800	Rect
3	3	6		√	Hammer	0 – 400	800	Rect
13	12	25	√		Hammer	0 - 200	400	Rect
13	12	25		√	Hammer	0 - 200	400	Rect
40	40	80	√		Hammer	0 – 80	200	Rect
40	40	80		√	Hammer	0 – 80	200	Rect
50	50	100	√		Liquidator	4 – 30	100	Hanning
150	150	300	√		Liquidator	3 – 12	60	Hanning
200	200	400	√		Liquidator	2 - 10	50	Hanning

* S-R1: Distance from source to first receiver
# R1-R2: Distance from first receiver to second receiver
Δ R2-R3: Distance from second receiver to third receiver

Distances between receivers ranging from 3 to 400 ft were generally used (see Table 2). Typically, 10 receiver spacings were used at the test sites. The largest receiver spacing was typically based on space considerations and the energy level delivered by the seismic source. This number and progression of receiver spacings resulted in significant overlapping of the individual dispersion curves used to develop a composite field curve, thereby enhancing the test reliability and allowing the assumption of lateral uniformity over the test array to be studied. Regardless of the spacing between receivers, at no point in the data analysis were wavelengths considered that were longer than twice the distance between the source and first receiver in the receiver pair. This array geometry results in minimizing near-field effects while simultaneously recording long wavelengths.

Vertical velocity transducers were used as receivers. All tests were conducted with Mark Products Model L-4C transducers, which have a natural frequency of 1 Hz. An example of one L-4C receiver being placed in the field is presented in Figure 9. All three, 1-Hz geophones at one receiver set-up (see Figure 7) used at SASW Site No.2 of the Kingston Project Site is shown in Figure 10. The key points with regard to these receivers are that: (1) they have significant output over the primary measurement frequency range at the Kingston site(2 Hz to 400 Hz), (2) they are matched so that any differences in phase are negligible over the measurement frequency range, (3) they are coupled well to the soil, (4) the coupling is similar for each receiver, and (5) ambient temperatures were low enough (below 90°F) so as not to impact geophone performance. These 1-Hz geophones have outputs in excess of 10 volts/(in./sec) and phase shifts between receivers of less than 9 degrees for frequencies from 2 Hz to 400 Hz, the range used in testing with these receivers.

Figure 8 Photograph of Liquidator (from http://nees.utexas.edu/Home.shtml)

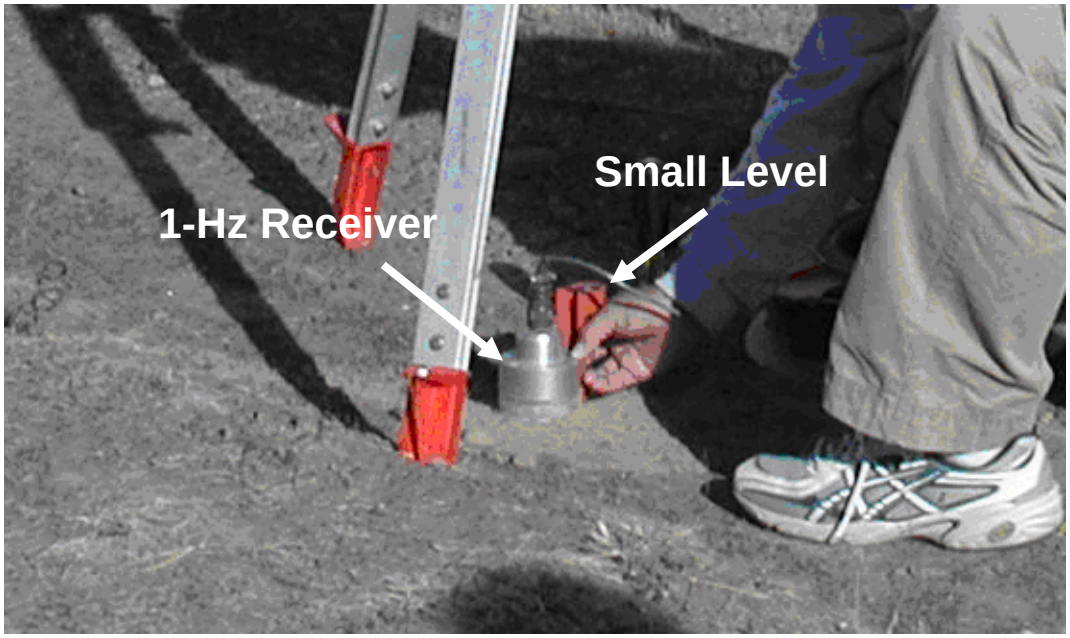

Figure 9 Photograph of 1-Hz Geophone Semi-Embedded in the Ground and the Pre-Test Check for Plumbness (Illustrative Photograph taken at Hanford, WA)

Figure 10 Photograph of Three, 1-Hz Geophones at one Receiver Set-up; SASW Site No. 2 at the Kingston Fly Ash Recovery Project.

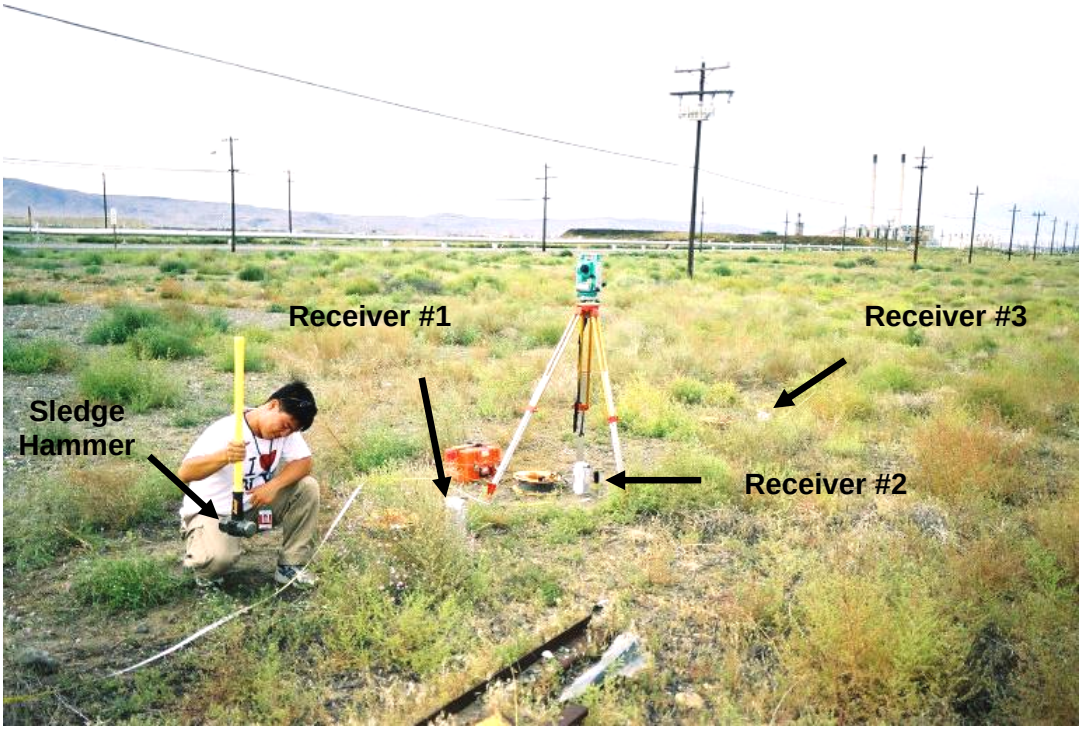

Figure 11 Photograph of Personnel Using the Sledge Hammer Source at Hanford, WA

The two types of seismic sources that were used to generate energy over the required frequency ranges at the test sites were hand-held hammers and a Liquidator. At the shorter receiver spacings (typically 3 to 25 ft), a sledge hammer was employed as illustrated in Figure 11. For receiver spacings equal to and greater than 50 ft, Liquidator, a vibroseis that is owned and operated by The University of Texas at Austin (UT) was used. Figure 12 is a photograph of Liquidator working at the Kingston Project at SASW Site No.5. Liquidator is an excellent source for SASW tests that require profiling depths of 300 ft or greater.

The recording device used in these tests was a Dataphysics Quattro Dynamic Signal Analyzer, a four-channel analyzer. The dynamic signal analyzer was used to record the geophone output and to perform calculations in the frequency domain so that the relative phase of the cross-power spectrum (discussed below) could be reviewed in the field during data collection. In addition, the source output from the analyzer was used to control the vibration frequency and amplitude of Liquidator. SASW tests with Liquidator were performed in a stepped-sine mode (from high to low frequencies at the Kingston site), where the source signal was swept over the frequencies of interest and the relative phase was determined at each frequency. This process also allowed the operator to evaluate subjectively the data being collected in the field to assure consistency with the expected Rayleigh wave propagation in a layered halfspace.

3.2 Spectral Calculations

The dynamic signal analyzer was used to measure time-domain records (x(t) and y(t)) from the two receivers in each receiver pair at each receiver spacing. These time records were then transformed into Laplace form X(s) and Y(s). Then the output is related to the input by the transfer function H(s):

$$X(s) = \mathcal{L}\{x(t)\} \stackrel{\text{def}}{=} \int_{-\infty}^{\infty} x(t)e^{-st}\,dt \tag{2}$$

$$Y(s) = \mathcal{L}\{y(t)\} \stackrel{\text{def}}{=} \int_{-\infty}^{\infty} y(t)e^{-st}\,dt \tag{3}$$

$$H(s) = \frac{Y(s)}{X(s)} \tag{4}$$

$$G(\omega) = \frac{|Y|}{|X|} = |H(j\omega)| \tag{5}$$

Figure 12 Photograph of Liquidator Working at SASW Site No. 5 of the Kingston Fly Ash Recovery Project

$$\phi(\omega) = \arg(Y) - \arg(X) = \arg(H(j\omega)) \quad (6)$$

In a linear time-invariant system, the input circular frequency, ω, has not changed. Only the amplitude and phase angle of the sinusoid has been changed by the system. This change for every circular frequency, ω, is described by the frequency response $H(j\omega)$. The phase shift between two receivers is given by $\phi(\omega)$.

The phase shift calculated from the transfer function, $\phi(\omega)$, is the key spectral quantity in SASW testing. When the sledge hammer was used as the source, the spectral functions were determined by comparing the Fast Fourier Transform (FFT) of geophone signals in a certain frequency range. When Liquidator was used as the source, the spectral functions were determined one frequency at a time in a stepped-sine fashion (Stokoe et al., 2006). The number of averages and integration time were adjusted in the field to control how long the source remained at each frequency. Typically five or more averages were used at each frequency in the determination of the spectral functions when Liquidator was used as the source. Ten averages were typically used when the impact source (sledge hammer) was employed. The phase shift calculated from the transfer function, simply called the phase hereafter, represents the phase difference of the motion at the two receivers. One set of spectral functions was measured for each receiver spacing and testing direction.

As an example, a wrapped phase spectrum from one receiver spacing is shown in Figure 12a. For these measurements, Liquidator was the source and the data were collected with a 50-ft receiver spacing at Site 5. Construction of individual dispersion curves from each receiver pair and combining them into composite dispersion curves are discussed below.

3.3 Data Reduction and Forward Modeling Procedure

The data collected in the field, in the form of phase plots, were transferred from the original laptop hard disk that was connected to the analyzer in the field to a desktop computer for analysis. The data were then reduced and interpreted using the program WinSASW. This program was developed by Professor Sung Ho Joh at the University of Texas at Austin (Joh, 1996).

3.3.1 Constructing Individual and Composite Field Dispersion Curves

Data reduction consisted of the following steps. For each spacing associated with a receiver pair, the phase plot was loaded into WinSASW. Figure 13a shows the wrapped phase collected with Liquidator and a 50-ft, S-R#1 receiver spacing at SASW Site No. 5. A masking procedure was then performed to manually eliminate portions of the data with poor signal quality and/or portions of the data contaminated by near-field waveform components. Figure 13b shows the masking applied to the original wrapped phase plot in Figure 13a. The WinSASW program uses the masking information to unwrap the phase plot, and then calculate the individual dispersion curve using the relationship presented in Equation 1.

As an example of the process followed in constructing an individual dispersion curve, consider Points #1 and #2 in Figure 13b which were measured using Liquidator as the source. Points #1 and #2 represent seismic waves with one and two wavelengths between the receiver pair that had receivers located at 50 and 100 ft from Liquidator. The unwrapped phase angles are 360° (one wavelength) and 720°(two wavelengths) for Points #1 and #2, respectively. The frequencies associated with Points #1 and #2 are 9.6 and 17.9 Hz, respectively, which results in phase velocities of 480fps (9.6*50ft) and 448fps (17.9*25ft), respectively. The complete individual dispersion curve calculated from the unmasked portion of the wrapped phase record in Figure 13b is shown in Figure 14. This process is repeated for all receiver spacings which results in a composite experimental field dispersion curve that covers a wide range of wavelengths. Figure 15 shows the composite experimental dispersion curve created at Site No. 5, first with the sledge hammer and then with Liquidator as the seismic sources. The maximum wavelength, λ_{max}, measured at Site 5 was 611 ft. This wavelength was measured with S-R2 = 300 ft and R2 - R3 = 300 ft. The maximum depth to which the V_s profile was determined with Liquidator at this site is λ_{max} /2 or 306 ft as discussed below.

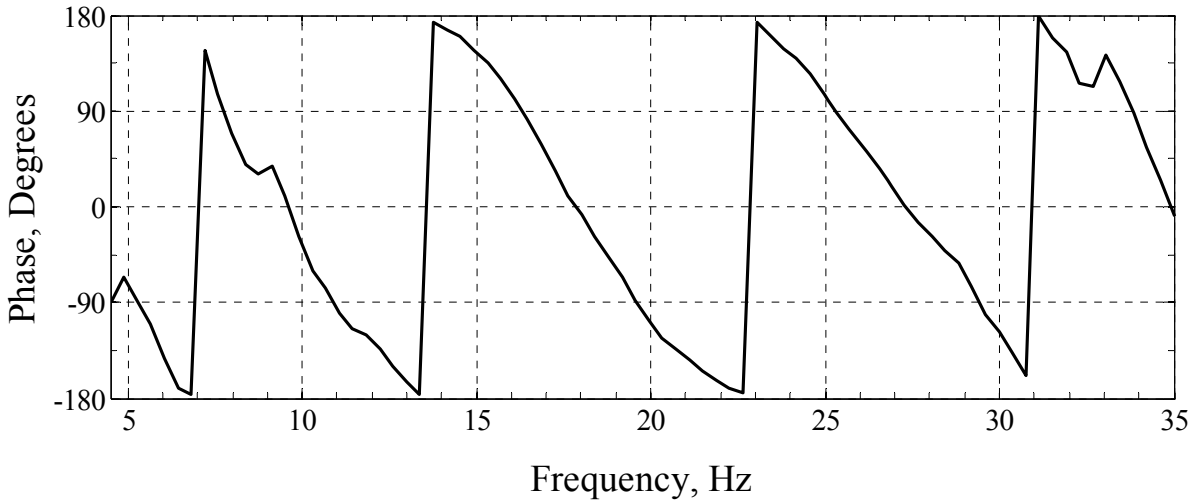

a. Wrapped Phase Calculated from Transfer Function

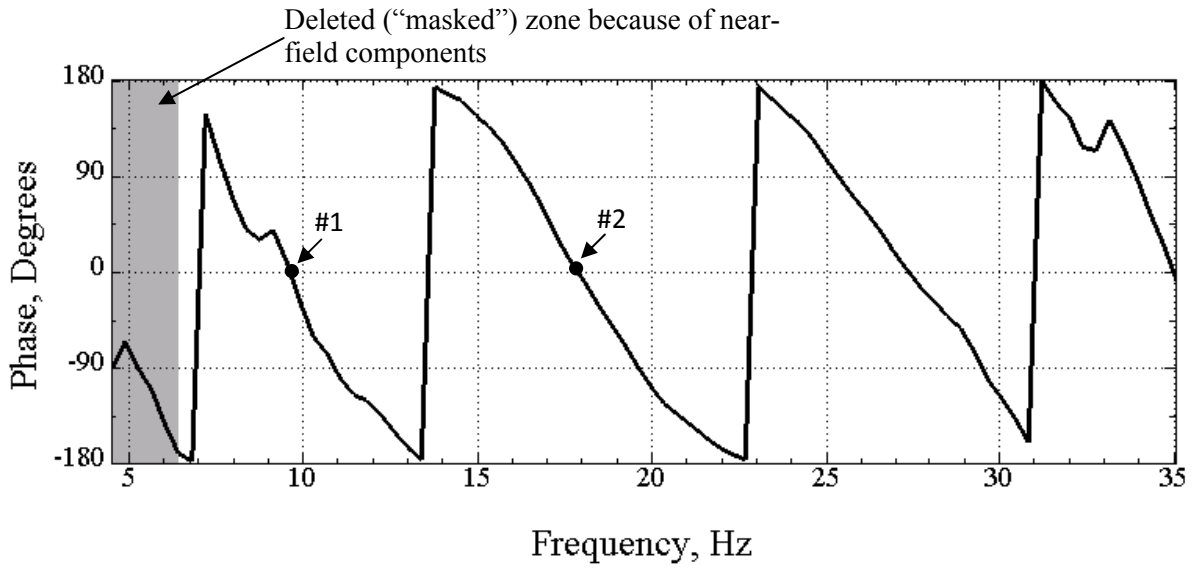

b. Masked Wrapped Phase to Minimize Near-Field Components

Figure 13 Wrapepd Phase of the Transfer Function Measured at SASW Site No. 5 with Liquidator as the Seismic Source and a 50-ft, S-R#1 Receiver Spacing

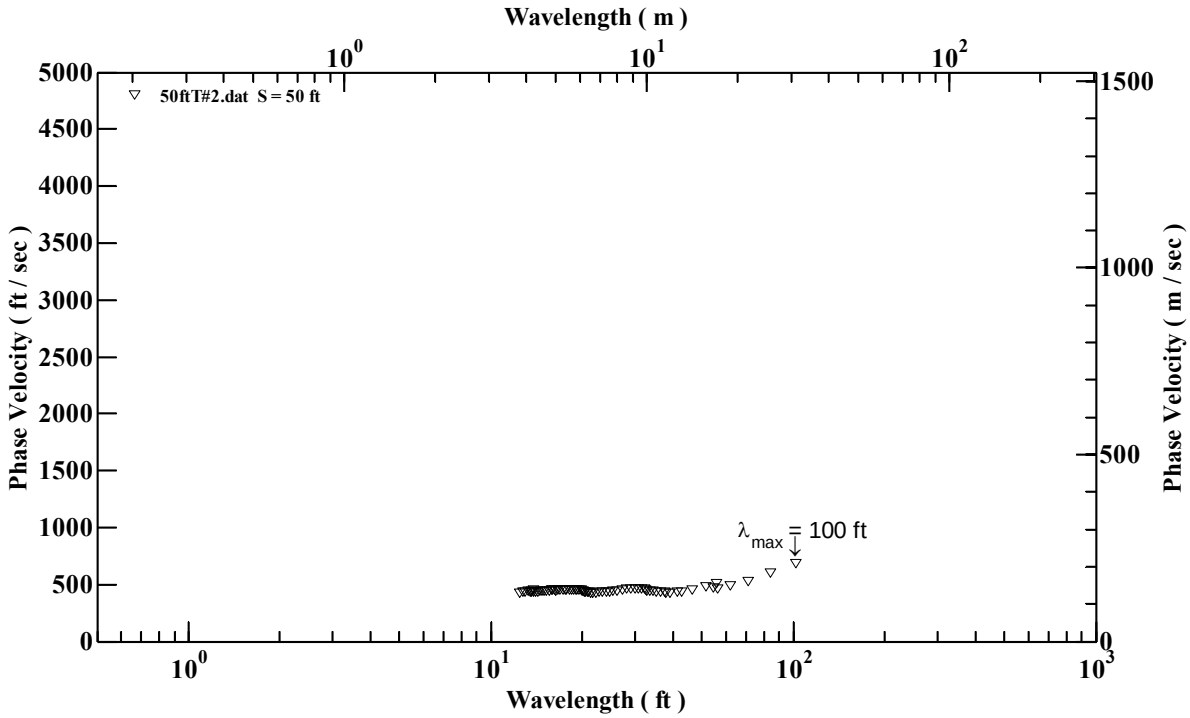

Figure 14 Individual Experimental Dispersion Curve Created from the Unwrapped Phase Record in Figure 13b Measured with a 50-ft Receiver Spacing (50 ft between the Receiver Pair) at SASW Site No. 5

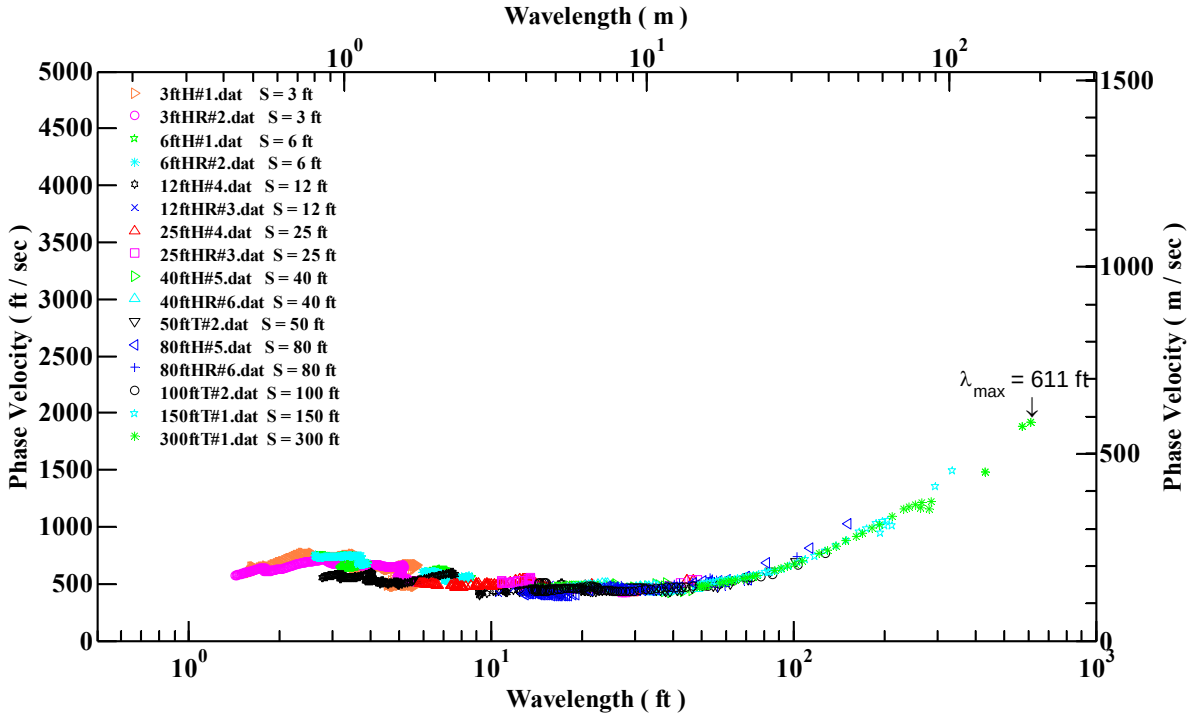

Figure 15 Composite Experimental Dispersion Curve Created from Phase Measurements Performed at all Receiver Spacings at SASW Site No. 5 using the Sledge Hammer and Liquidator as the Seismic Sources

3.3.2 Matching the Composite Field and Theoretical Dispersion Curves

The next step in the data reduction process is the creation of a theoretical dispersion curve which matches the field dispersion curve. The software program WinSASW is used for this purpose. WinSASW uses an algorithm developed by Professor Jose Roesset using the stiffness matrix approach to generate a theoretical dispersion curve for a given shear wave velocity profile (Kausel and Roesset, 1981). The theoretical dispersion curve is generated using either the first-mode Rayleigh wave solution (termed 2D approach) or a complete solution that includes all modes and both surface and body waves (termed 3D approach) (Foinquinos, 1991, and Roesset et al, 1991). For these analyses, the more accurate 3D approach was employed. With this approach, an initial shear wave velocity profile is first assumed based on the characteristics of the measured experimental dispersion curve. The theoretical dispersion curve is generated and compared with the experimental curve. The features of the shear wave velocity profile (shear wave velocities and layer thicknesses) are iteratively changed until an acceptable fit to the experimental curve is achieved. The goodness of the fit is based on visually determining a best fit which, in this study, was based on Mr. Yuan's judgment followed by a review by Professor Stokoe.

The matching process is shown herein using the composite experimental dispersion curve for SASW Site No. 5 that is presented in Figure 15. The theoretical dispersion curve which is considered to match (best fit) this composite field dispersion curve is shown in Figure 16. The shear wave velocity profile for the site is presented in Figure 17. The parameters used to generate the theoretical dispersion curve in Figure 17 are listed in Table 3. As shown in Figure 17, the maximum profile depth is λ_{max} /2 which is 306 ft.

3.3.3 Additional Considerations

To generate the theoretical dispersion curves used to match the field dispersion curves, some assumptions have to be made. First, the unit weight and Poisson's ratio of the material must be assumed. Above the water table, Poisson's ratio was based on the V_s values determined in the forward modeling process. If the V_s value was between 0 and 2500 fps, Poisson's ratio was taken to be 0.33. However, if the soil layer was below the water table, the value of Poisson's ratio was determined by assuming V_p to be 5000 fps and calculating Poisson's ratio based on the assumed V_s and V_p (5000 fps) values. For V_s values above 3000 fps, Poisson's ratio is assumed

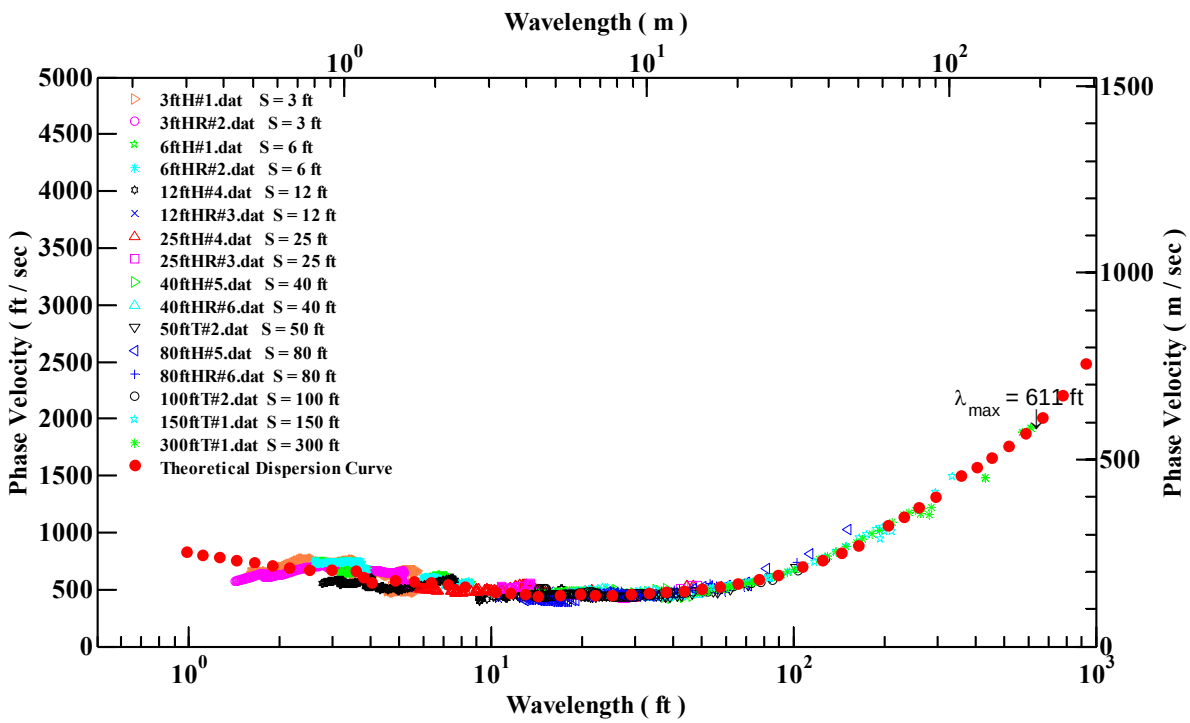

Figure 16 Comparison of the Fit of the Theoretical Dispersion Curve to the Composite Experimental Dispersion Curve at SASW Site No. 5

Table 3 Parameters Used to Obtain the V_S Profile at SASW Site No. 5, Kingston Fly Ash Recovery Project, Harriman, TN

Layer No.	Thickness, ft	Depth to Top of Layer, ft	P-Wave Velocity, ft/s	S-Wave Velocity, ft/s	Assumed Poisson's Ratio	Assumed Total Unit Weight, pcf
1	0.5	0	1965	990	0.33	110
2	2.5	0.5	1290	650	0.33	110
3	6	3	754	380	0.33	110
4	12	9	933	470	0.33	110
5	29	21[◊]	5000	600	0.49[+]	110
6	50	50	5000	1120	0.47[+]	110
7	50	100	5000	2700	0.29[+]	135
8[*]	99999	150	6062	3500	0.25	135

* Layer extends below maximum depth of the V_s Profile.
◊ Water table assumed at a depth of 21 ft
\+ Not assumed but back-calculated from V_p = 5000 fps and V_s

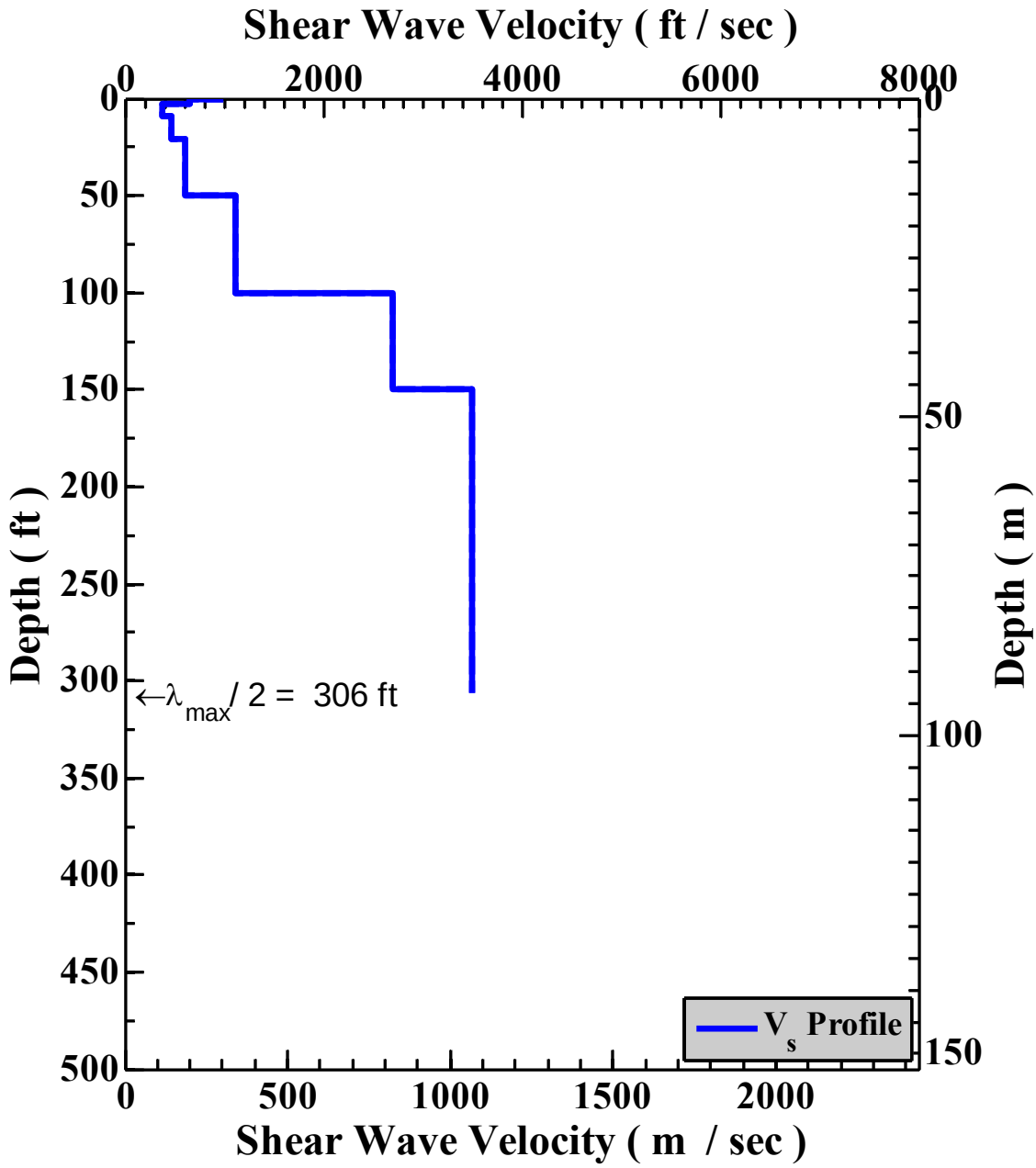

Figure 17 Final Shear Wave Velocity Profile Determined at SASW Site No. 5

to be 0.25 since the material skeleton rather than water dominates the compression wave velocity. This calculation of Poisson's ratio was performed in WinSASW once the layer was designated as being below the water table. It should be noted that the depths of the water table for the nine sites were assumed based on information from personnel at Stantec Consulting Services using existing borings and wells.

The unit weights assumed in this study were also based on the V_s values. Generally, if V_s was between 0 and 1500 fps, the unit weight was assumed to be 110 pcf. If V_s was between 1500 and 2500 fps, the unit weight was assumed to be 120 pcf. If V_s was greater than 2500 fps and below water table, the unit weight was assumed to be 135 pcf.

Theoretical dispersion curves can also be generated using different assumptions of receiver locations. For these analyses, the theoretical dispersion curve was calculated assuming Source-to-Receiver #1 spacing of two wavelengths, and Source-to-Receiver #2 spacing of four wavelengths. These receiver locations represent far-field motions. Past studies have shown that the range in wavelengths collected in the SASW test does not differ significantly from the far-field motions (Foinquinos, 1991; Roesset et al, 1991; Sanchez-Salinero, 1987; and Jathal, 2003).

Lastly, the final shear wave velocity profile is presented to a depth of approximately 0.5 times the maximum wavelength (λ_{max} /2) in the experimental dispersion curve. This cutoff depth is based on the fact that most of the particle motion occurs at depths less than one-half of the wavelength, as shown in Figure 2. Past experience has shown this maximum depth to be an acceptable cut-off depth for most shear wave velocity profiles.

4. Discussion of the V_s Profiles

Each V_s profile at the nine SASW test sites is presented in tabular and graphical forms in Appendices A and B, respectively. The profiling depths range from a minimum of 193 ft at Site No. 9 to a maximum of 405 ft at Site No. 1. The profiling depths were primarily controlled by: (1) the overall site stiffness, (2) the thickness and stiffness of the soil over the bedrock, (3) the velocity contrast between the soil and bedrock and (4) the extent of available space at the site over which to locate a linear source-receiver array. For instance, the deepest profile was at Site No. 1 which is composed of rock nearly to the surface (hence, the stiffest site) and had enough space to permit an 800-ft long S-R$^{\#}$3 array to be used.

Each V_s profile has also been interpreted to estimate the geologic profile at the site. These interpreted profiles are present in Appendix C. To assist in the interpretation, estimated V_s profiles for a medium dense sand and a dense gravel were added to each profile to a depth of 150 ft. These "soil" V_s profiles were simply used as relative values.

Upon reviewing the interpreted V_s profiles, the profiles can be divided into three groups as follows:

Group 1: Shale extending nearly to the surface.

Only one site, Site No. 1, exhibits this profile. The profile was interpreted as weathered shale over unweathered shale over a stiffer rock.

Group 2: Soil over shale.

Six sites exhibit this profile. The sites are Nos. 3, 4, 5, 6, 7, and 8, with only Site No. 8 exhibiting about a 25-ft thick layer of weathered shale on top of unweathered shale. Based on these and the other sites, the weathered shale was assumed to exhibit V_s in the range of 1650 to 2200 fps and the unweathered shale to exhibit V_s in the range of 2500 to 3500 fps.

Group 3: Soil over weathered shale.

Two sites, Nos. 2 and 9, exhibit soil over weathered shale, where the weathered shale is more than 100 ft thick.

With the interpreted profiles, the depths to the top of the unweathered shale were estimated and the median shear wave velocity profile in the unweathered shale was calculated. The estimated depths to the top of the unweathered shale are:

Site No. :	1	2	3	4	5	6	7	8	9
Estimated Depth (ft):	10	290	74	78	100	90	55	74	>200

The median V_s profile of the unweathered shale is presented in Figure 18, including the 16th and 84th percentiles, the coefficient of variation (COV) and the number of profiles. The COV is less than 0.2. The median V_s in the top 150 ft of the unweathered shale increases slightly with depth, ranging from about 2700 to 3000 fps. Below 150 ft, the median value of V_s in the unweathered shale jumps to about 3500 fps over the next 50 ft. However, this median value is based on five or fewer profiles.

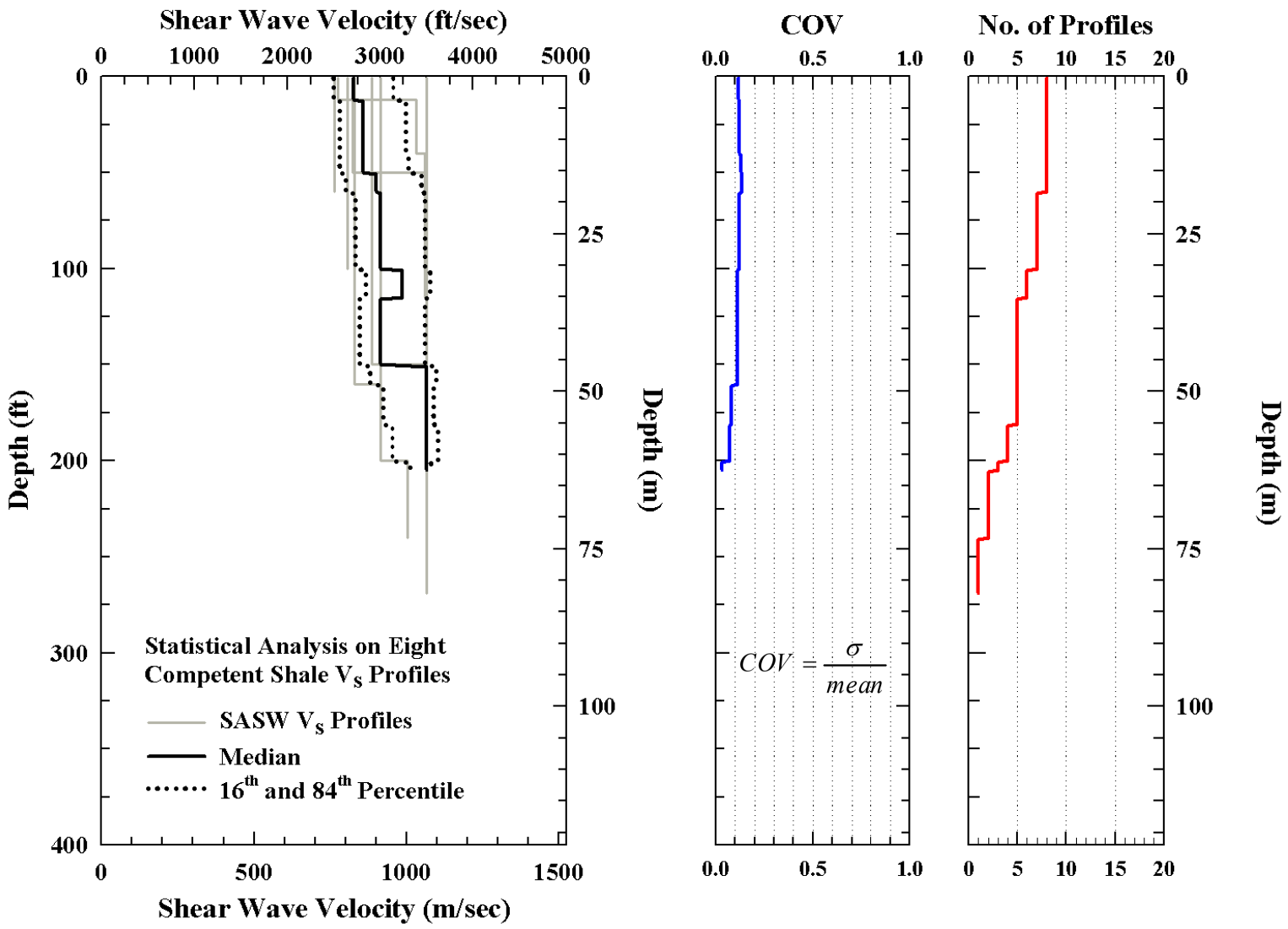

Figure 18 Statistical Analysis of V_S Profiles of the Unweathered Shale Indentified in the Interpreted Profiles in Appendix C

5. Summary and Conclusions

Nine (9) sites at the location of the Kingston Fly Ash Recovery Project were seismically tested using the SASW method. The main purpose of the seismic tests was to determine shear wave velocity, V_s, profiles in the upper shale bedrock at Kingston Project Site. An overview of the SASW method and associated field testing and data analysis procedures are briefly presented. Field data collected at SASW Site No. 5 are used to illustrate the field and analysis procedures.

The V_s profiles at the nine test sites were analyzed to study: (1) the V_s profiles in the soil above the bedrock, (2) the depth to bedrock, and (3) V_s profiles in the shale bedrock and beneath. The V_s profiles are presented in Appendices A and B in tabular and graphical forms, respectively. The profiling depths ranged from 193 ft at Site No. 9 to 405 ft at Site No. 1. The field testing progressed smoothly and data analysis to develop the V_s profiles was straightforward.

The nine V_s profiles were interpreted to estimate the material profile at each site. The interpreted profiles are presented in Appendix C. Of the nine sites, six sites (Nos. 3, 4, 5, 6, 7 and 8) were interpreted to show soil over shale bedrock. Site No. 1 showed shale coming almost to the ground surface. At this site, the shale was underlain by stiffer rock. Sites No. 2 and 9 were interpreted to be composed of soil over deeply weathered shale.

In terms of depth to the top of unweathered shale, this depth ranged significantly around the Kingston Fly Ash Recovery Project from 10 ft (Site No. 1) to 290 ft (Site No. 2) as discussed in Section 4. The weathered shale, based on the interpreted profiles of Sites No. 1, 2, 8 and 9, exhibited V_s values in the range of 1650 to 2200 fps. The unweathered shale exhibited V_s values in the range of 2500 to 3500 fps, based on the interpreted profiles of Sites No. 1, 2, 3, 4, 5, 6, 7 and 8. (The unweathered shale was not encountered within the profiling depth of 193 ft at Site No. 9.) A statistical analysis of the V_s profiles in the unweathered shale is presented in Figure 18.

6. References

1. Foinquinos, M.R., (1991), "Analytical Study of Inversion for the Spectral Analysis of Surface Waves Method," Master's Thesis, The University of Texas at Austin, 119 pgs.

2. Fuhriman, M.D. and Stokoe, K.H., II (1993), "Crosshole Seismic Test at the Gilroy No. 2 and Treasure Island Sites Affected by the 1989 Loma Prieta Earthquake," Geotechnical Engineering Report GR93-1, Civil Engineering Department, University of Texas at Austin, Austin, TX, January, 259 pgs.

3. Jathal, J.K. (2003), "Investigation of V_s Profiles Measured by Borehole and Surface-Wave Seismic Techniques," Thesis, The University of Texas at Austin, 348 pgs.

4. Joh, S.-H. (1996), "Advances in the Data Interpretation Technique for Spectral- Analysis-of-Surface-Waves (SASW) Measurements," Ph.D. Dissertation, The University of Texas at Austin, 240 pgs.

5. Kausel, E. and Roesset, J.M. (1981), "Stiffness Matrices for Layered Soils," *Bulletin of the Seismological Society of America*, 71, pp. 1743-1761.

6. Roesset, J.M., Chang D.-W., and Stokoe, K.H., II (1991), "Comparison of 2D and 3D Models for Analysis of Surface Wave Tests," *Proceedings of the 5th International Conference on Soil Dynamics and Earthquake Engineering*, pp. 111-126.

7. Sanchez-Salinero, I. (1987), "Analytical Investigation of Seismic Methods used for Engineering Applications," Ph.D. Dissertation, The University of Texas at Austin, 401 pgs.

8. Stokoe, K.H., Cox, B.R., Lin, Y.-C., Jung, M.J., Menq, F.-Y., Bay, J.A., Rosenblad, B., and Wong, I. (2006). "Use of Intermediate to Large Vibrators as Surface Wave Sources to Evaluate V_s Profiles for Earthquake Studies," 19th Symposium on the Application of Geophysics to Engineering and Environmental Problems, Seattle, WA, 18 pgs.

9. Stokoe, II, K.H., Lin, Y.C., Cox, B., Kurtulus, A., Jung, M.J. (2005). "Shear Wave Profiling at the Waste Treatment Plant Site, Hanford, WA," Vols. I and II, Geotechnical Engineering Report GR05-1, University of Texas at Austin, July, 243 pgs.

10. Stokoe, K.H., II, Wright, S.G., Bay, J.A. and J.M. Roesset (1994), "Characterization of Geotechnical Sites by SASW Method," *ISSMFE Technical Committee 10 for XIII ICSMFE*, Geophysical Characteristics of Sites, A.A. Balkema Publishers/Rotterdam & Brookfield, Netherlands, pp. 785-816.

Appendix A

Parameters Used to Obtain the V_s Profile of Each SASW Test Site at the Kingston Fly Ash Recovery Project, Harriman, TN

Table A.1 Parameter Used to Obtain the V_s Profile of Site 1 at the Kingston Fly Ash Recovery Project, TN

Layer No.	Thickness, ft	Depth to Top of Layer, ft	P-Wave Velocity, ft/s	S-Wave Velocity, ft/s	Assumed Poisson's Ratio	Assumed Total Unit Weight, pcf
1	2	0	2085	1050	0.33	110
2	3	2	3435	1730	0.33	120
3	5	5	4169	2100	0.33	120
4	12	10	4400	2540	0.25	135
5	28	22[◊]	5872	3390	0.25	135
6	75	50	6028	3480	0.25	135
7	120	125	8452	4880	0.25	135
8	210	245	10444	6030	0.25	135
9[*]	99999	455	11778	6800	0.25	135

[◊]Water table reported at a depth of 22 ft

[*]Layer extends below maximum depth of the V_s profile.

Table A.2 Parameter Used to Obtain the V_s Profile of Site 2 at the Kingston Fly Ash Recovery Project, TN

Layer No.	Thickness, ft	Depth to Top of Layer, ft	P-Wave Velocity, ft/s	S-Wave Velocity, ft/s	Assumed Poisson's Ratio	Assumed Total Unit Weight, pcf
1	1	0	735	370	0.33	110
2	2	1	854	430	0.33	110
3	4	3	1013	510	0.33	110
4	10	7	1231	620	0.33	110
5	43	17[◊]	5000	750	0.49[+]	110
6	30	60	5000	1220	0.47[+]	110
7	100	90	5000	1740	0.43[+]	120
8	100	190	5000	2200	0.38[+]	120
9[*]	99999	290	5000	2500	0.33[+]	135

[◊] Water table reported at a depth of 17 ft

[*] Layer extends below maximum depth of the V_s profile.

[+] Not assumed but back-calculated from V_p = 5000 fps and V_s

Table A.3 Parameter Used to Obtain the V_s Profile of Site 3 at the Kingston Fly Ash Recovery Project, TN

Layer No.	Thickness, ft	Depth to Top of Layer, ft	P-Wave Velocity, ft/s	S-Wave Velocity, ft/s	Assumed Poisson's Ratio	Assumed Total Unit Weight, pcf
1	1	0	1123	600	0.33	110
2	2	1	1478	790	0.33	110
3	4	3	1553	830	0.33	110
4	7	7	1459	780	0.33	110
5	60	14[◊]	5000	840	0.49[+]	110
6	150	74	5023	2900	0.25	135
7[*]	99999	224	6062	3500	0.25	135

[◊] Water table reported at a depth of 14 ft

[*] Layer extends below maximum depth of the V_s profile.

[+] Not assumed but back-calculated from V_p = 5000 fps and V_s

Table A.4 Parameter Used to Obtain the V_s Profile of Site 4 at the Kingston Fly Ash Recovery Project, TN

Layer No.	Thickness, ft	Depth to Top of Layer, ft	P-Wave Velocity, ft/s	S-Wave Velocity, ft/s	Assumed Poisson's Ratio	Assumed Total Unit Weight, pcf
1	1	0	854	430	0.33	110
2	2	1	1429	630	0.33	110
3	8	3	1568	780	0.33	110
4	19	11[◊]	5000	600	0.49[+]	110
5	48	30	5000	760	0.49[+]	110
6	160	78	5000	2720	0.29[+]	120
7[*]	99999	238	5196	3000	0.25	135

[◊] Water table reported at a depth of 11 ft

[*] Layer extends below maximum depth of the V_s profile.

[+] Not assumed but back-calculated from V_p = 5000 fps and V_s

Table A.5 Parameter Used to Obtain the V_s Profile of Site 5 at the Kingston Fly Ash Recovery Project, TN

Layer No.	Thickness, ft	Depth to Top of Layer, ft	P-Wave Velocity, ft/s	S-Wave Velocity, ft/s	Assumed Poisson's Ratio	Assumed Total Unit Weight, pcf
1	0.5	0	1965	990	0.33	110
2	2.5	0.5	1290	650	0.33	110
3	6	3	754	380	0.33	110
4	12	9	933	470	0.33	110
5	29	21[◊]	5000	600	0.49[+]	110
6	50	50	5000	1120	0.47[+]	110
7	50	100	5000	2700	0.29[+]	135
8[*]	99999	150	6062	3500	0.25	135

[◊]Water table reported at a depth of 21 ft

[*]Layer extends below maximum depth of the V_s profile.

[+]Not assumed but back-calculated from V_p = 5000 fps and V_s

Table A.6 Parameter Used to Obtain the V_s Profile of Site 6 at the Kingston Fly Ash Recovery Project, TN

Layer No.	Thickness, ft	Depth to Top of Layer, ft	P-Wave Velocity, ft/s	S-Wave Velocity, ft/s	Assumed Poisson's Ratio	Assumed Total Unit Weight, pcf
1	0.5	0	834	420	0.33	110
2	2.5	0.5	1013	510	0.33	110
3	6	3	1231	620	0.33	110
4	11	9	1350	680	0.33	110
5	20	20[◊]	5000	770	0.49[+]	110
6	50	40	5000	840	0.49[+]	110
7	200	90	6062	3500	0.25	135
8[*]	99999	290	6928	4000	0.25	135

[◊] Water table reported at a depth of 20 ft

[*] Layer extends below maximum depth of the V_s profile.

[+] Not assumed but back-calculated from V_p = 5000 fps and V_s

Table A.7 Parameter Used to Obtain the V_s Profile of Site 7 at the Kingston Fly Ash Recovery Project, TN

Layer No.	Thickness, ft	Depth to Top of Layer, ft	P-Wave Velocity, ft/s	S-Wave Velocity, ft/s	Assumed Poisson's Ratio	Assumed Total Unit Weight, pcf
1	0.5	0	1985	1000	0.33	110
2	6.5	0.5	2184	1100	0.33	110
3	2	7	1767	890	0.33	110
4	9	9	854	430	0.33	110
5	22	18[◊]	5000	630	0.49[+]	110
6	15	40	5000	800	0.49[+]	110
7	200	55	5196	3000	0.25	135
8[*]	99999	255	5716	3300	0.25	135

[◊] Water table reported at a depth of 18 ft

[*] Layer extends below maximum depth of the V_s profile.

[+] Not assumed but back-calculated from V_p = 5000 fps and V_s

Table A.8 Parameter Used to Obtain the V_s Profile of Site 8 at the Kingston Fly Ash Recovery Project, TN

Layer No.	Thickness, ft	Depth to Top of Layer, ft	P-Wave Velocity, ft/s	S-Wave Velocity, ft/s	Assumed Poisson's Ratio	Assumed Total Unit Weight, pcf
1	1	0	834	420	0.33	110
2	6	1	1429	720	0.33	110
3	11	7	1807	910	0.33	110
4	10	18[◊]	5000	610	0.49[+]	110
5	16	28	5000	940	0.48[+]	110
6	30	44	5000	1650	0.44[+]	120
7	100	74	5000	2640	0.31[+]	135
8	205	174	7448	4300	0.25	135
9[*]	99999	379	13856	8000	0.25	135

[◊]Water table reported at a depth of 18 ft

[*]Layer extends below maximum depth of the V_s profile.

[+]Not assumed but back-calculated from V_p = 5000 fps and V_s

Table A.9 Parameter Used to Obtain the V_s Profile of Site 9 at the Kingston Fly Ash Recovery Project, TN

Layer No.	Thickness, ft	Depth to Top of Layer, ft	P-Wave Velocity, ft/s	S-Wave Velocity, ft/s	Assumed Poisson's Ratio	Assumed Total Unit Weight, pcf
1	1	0	1072	540	0.33	110
2	6	1	1429	720	0.33	110
3	11	7	1807	910	0.33	110
4	20	18[◊]	5000	640	0.49[+]	110
5	46	38	5000	940	0.48[+]	110
6	180	84	5000	1650	0.44[+]	120
7[*]	100	264	5000	2640	0.31[+]	135
8[*]	200	364	7448	4300	0.25	135
9[*]	99999	564	13856	8000	0.25	135

[◊] Water table reported at a depth of 18 ft

[*] Layer extends below maximum depth of the V_s profile.

[+] Not assumed but back-calculated from V_p = 5000 fps and V_s

Appendix B

Individual V_s Profiles of the 9 SASW Test Sites at the Kingston Fly Ash Recovery Project, Harriman, TN

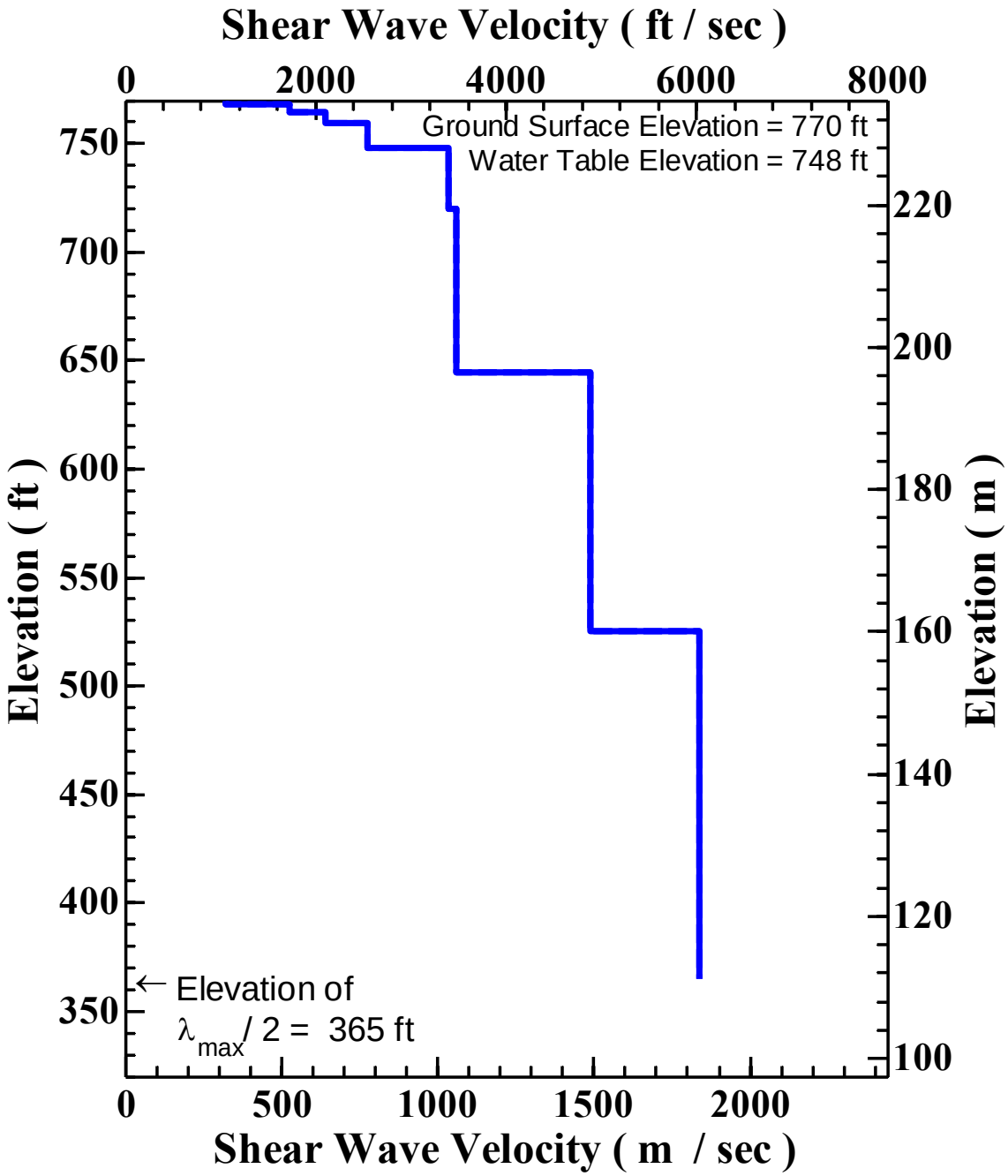

Figure B.1 Shear Wave Velocity Profile for Site 1

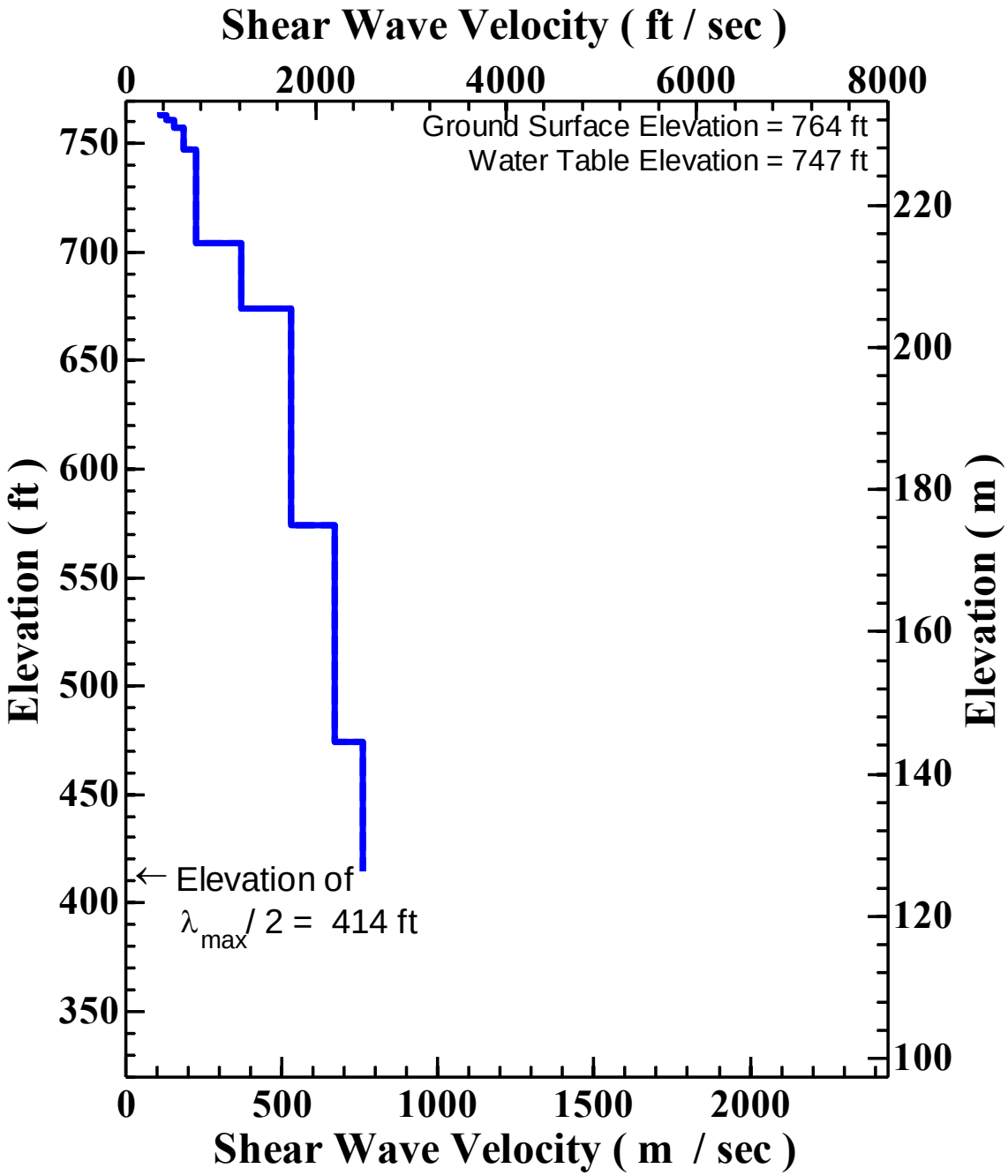

Figure B.2 Shear Wave Velocity Profile for Site 2

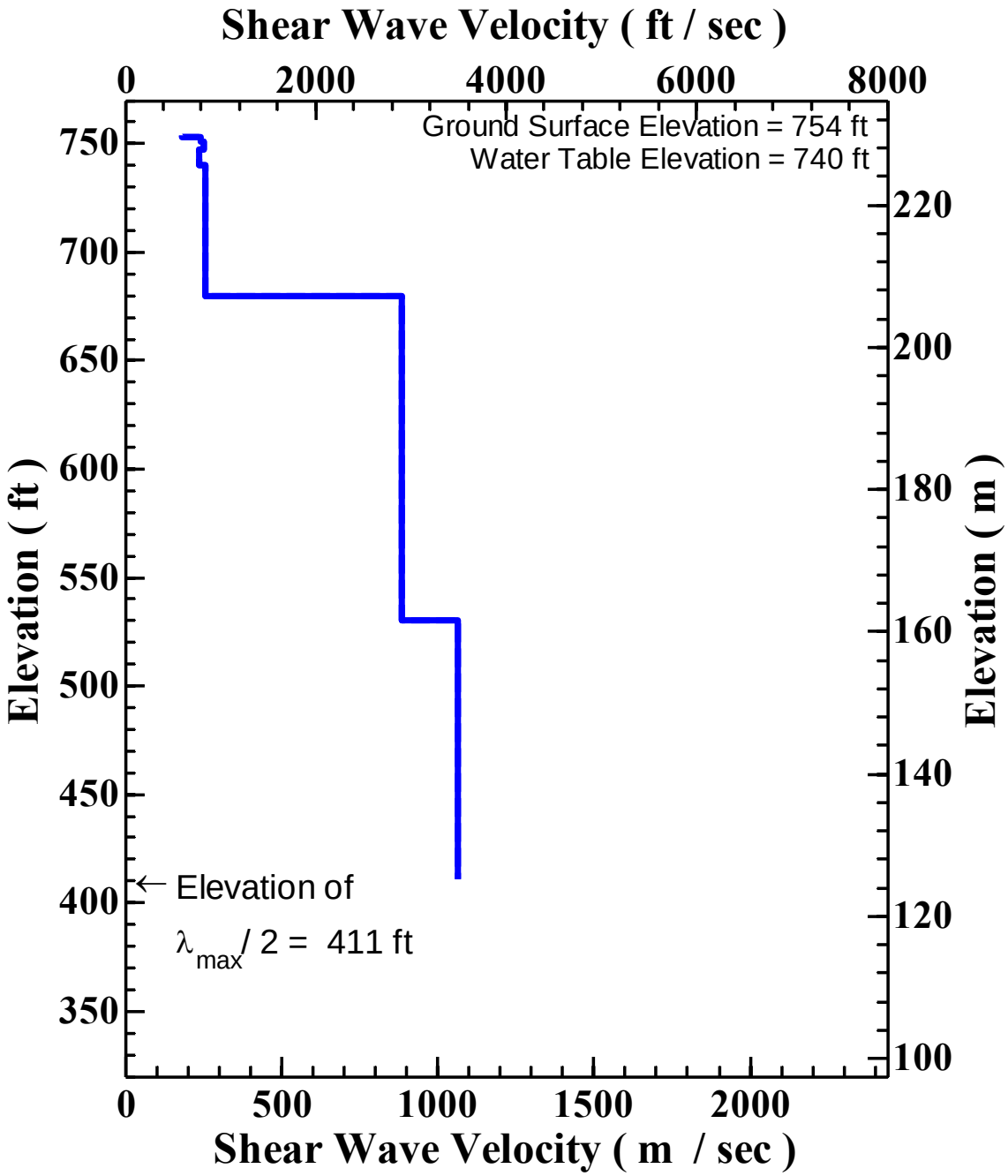

Figure B.3 Shear Wave Velocity Profile for Site 3

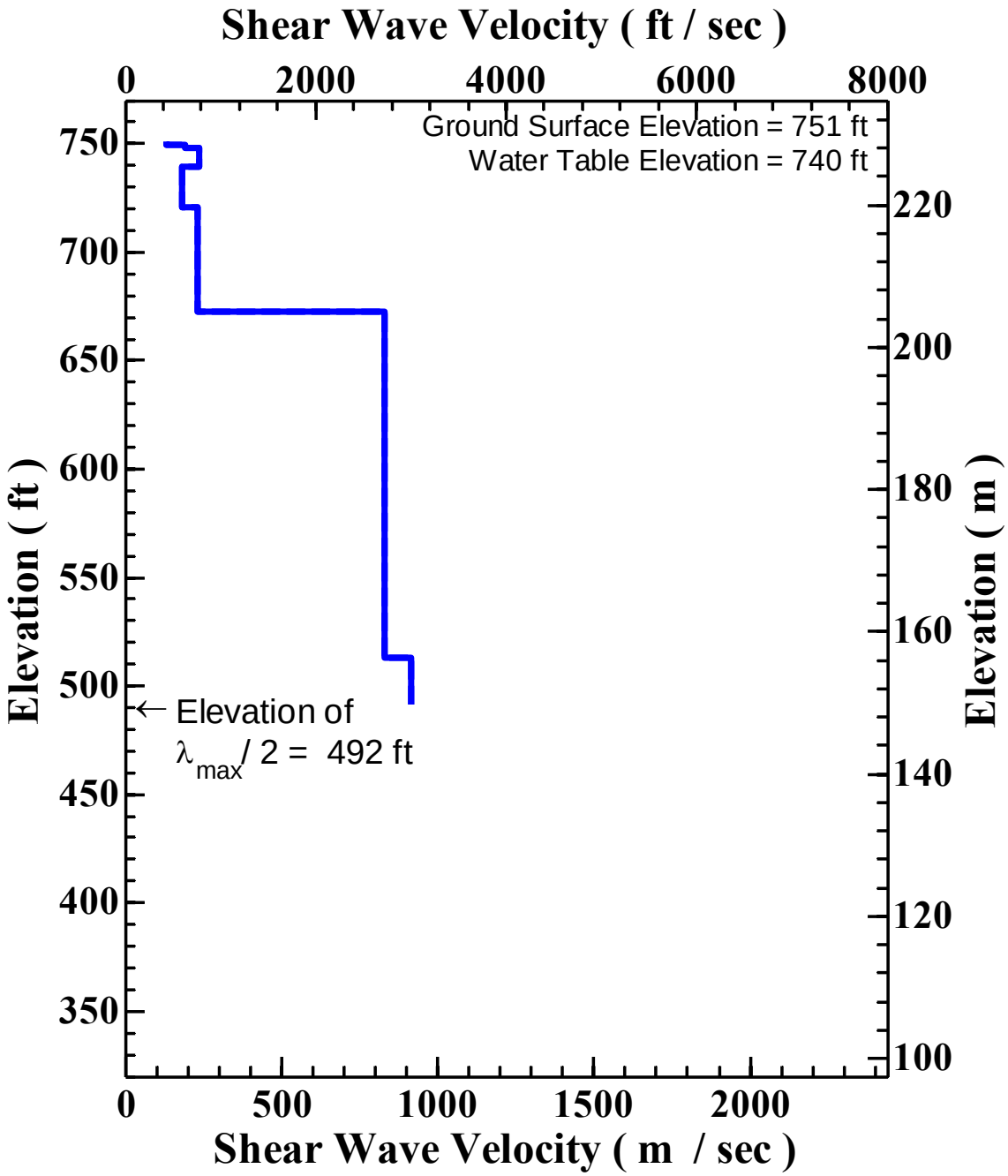

Figure B.4 Shear Wave Velocity Profile for Site 4

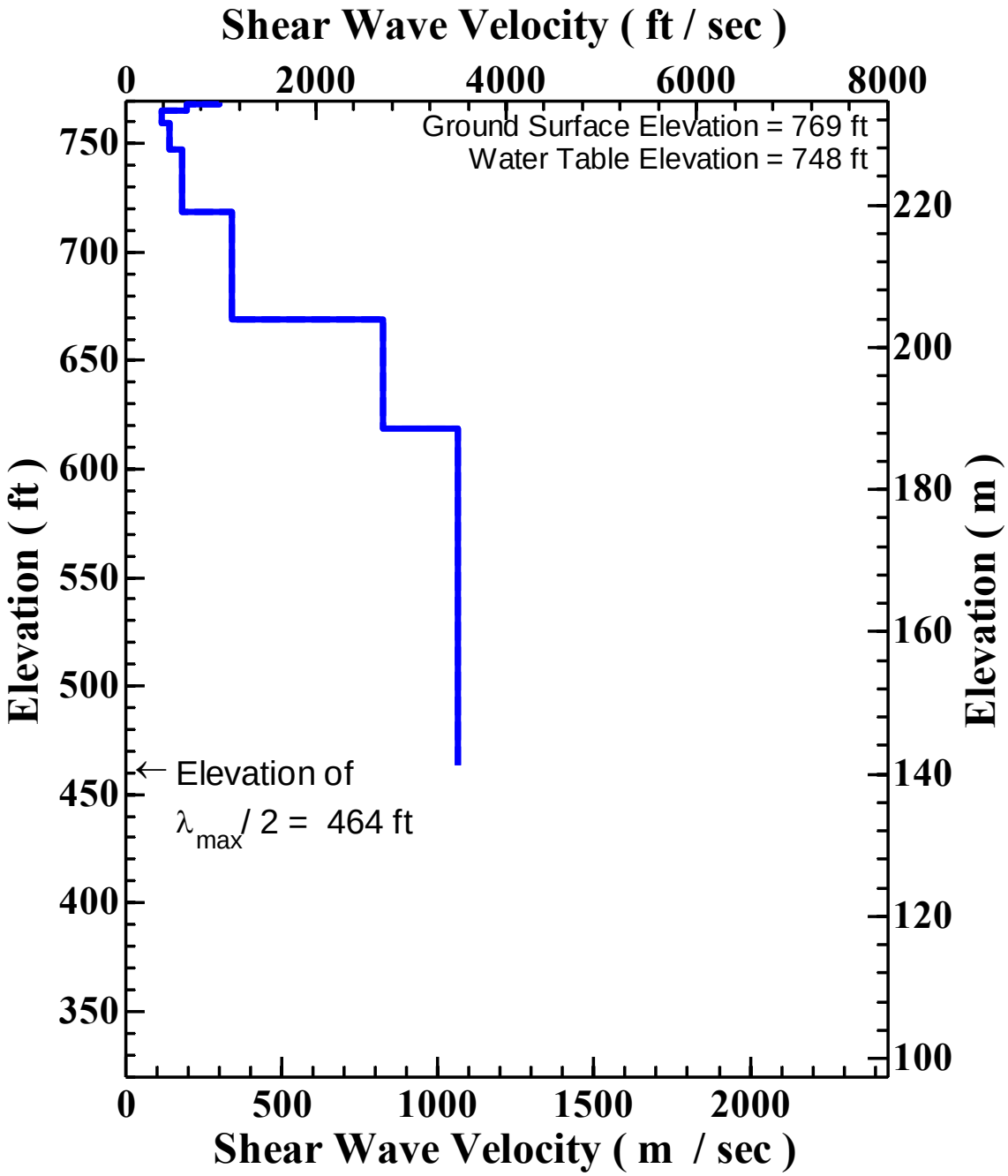

Figure B.5 Shear Wave Velocity Profile for Site 5

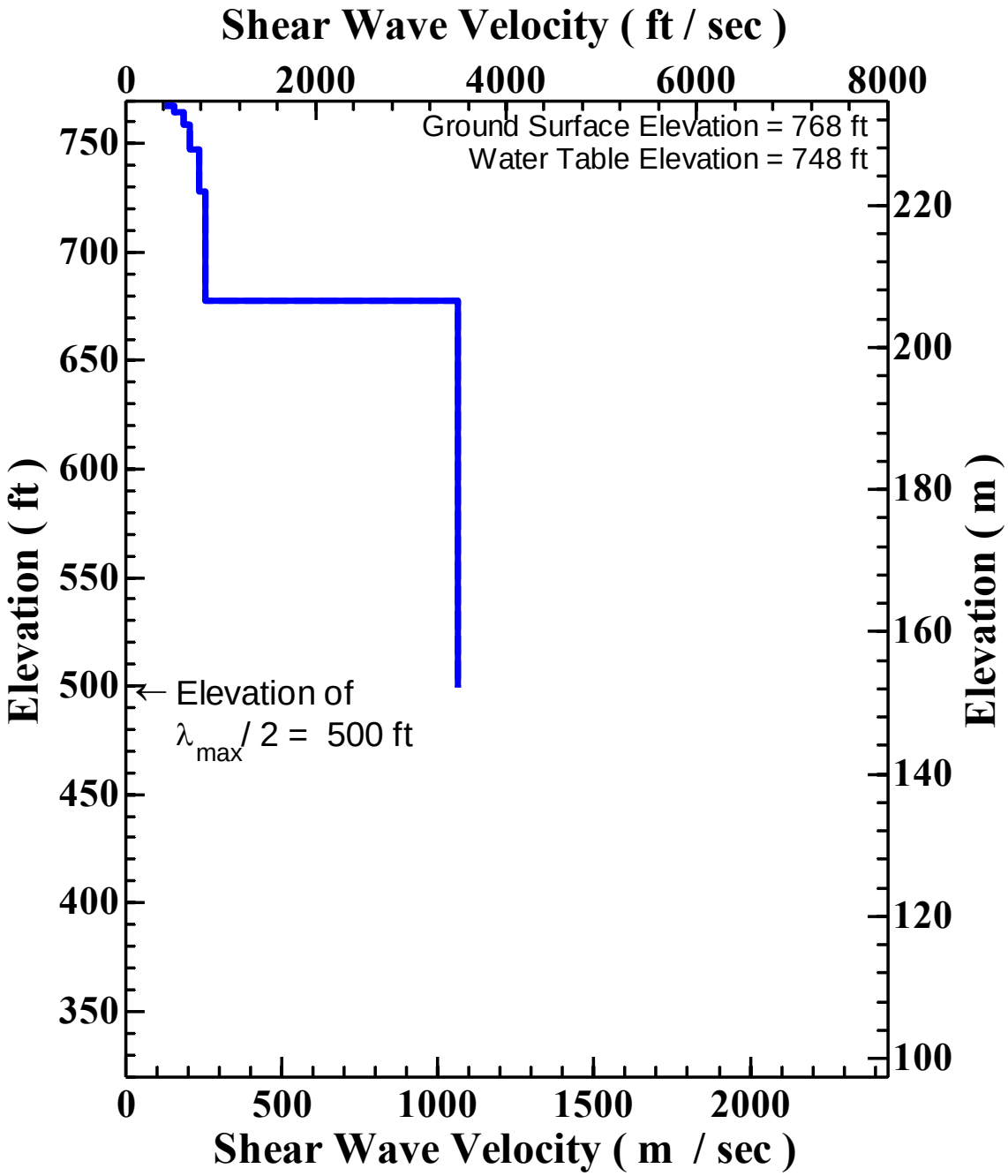

Figure B.6 Shear Wave Velocity Profile for Site 6

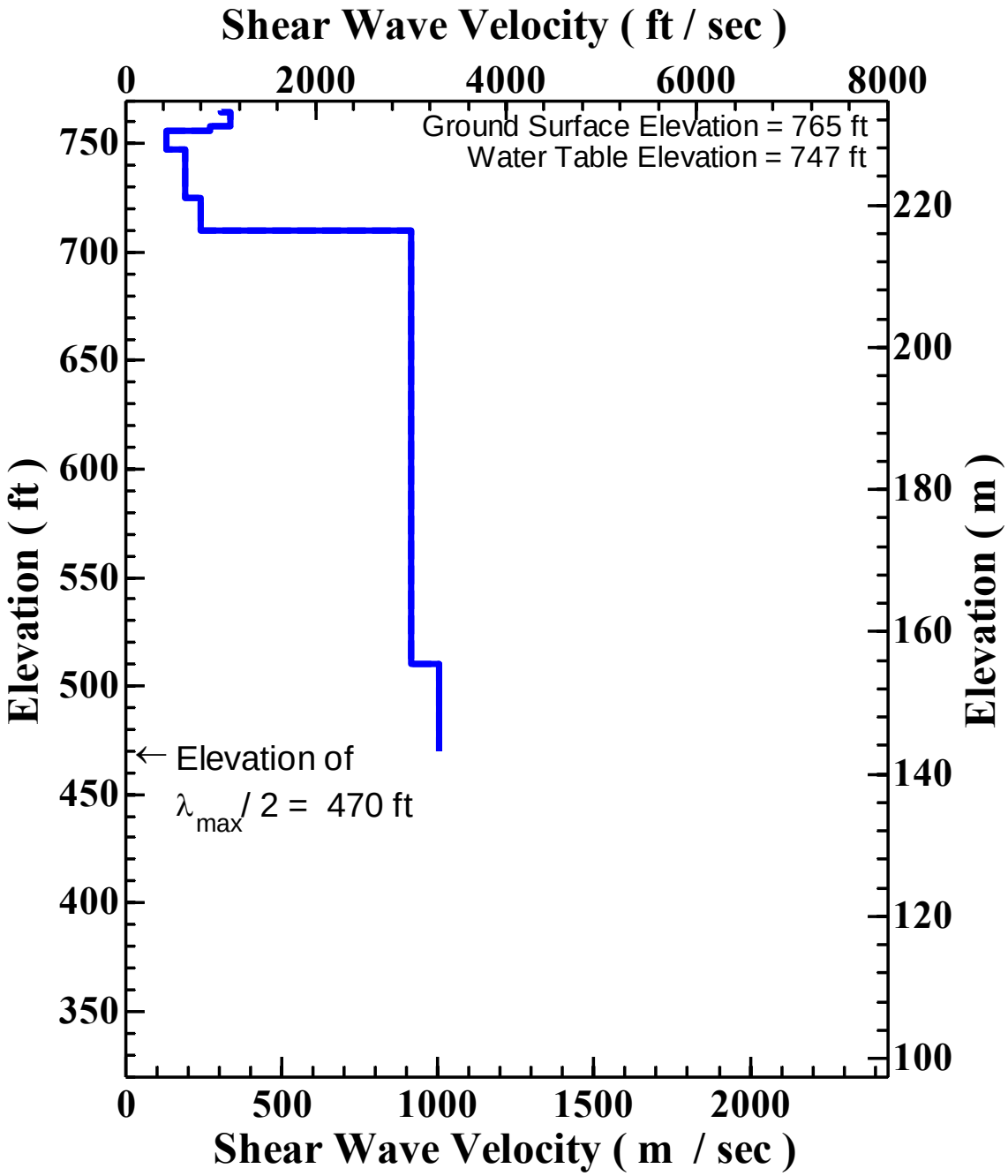

Figure B.7 Shear Wave Velocity Profile for Site 7

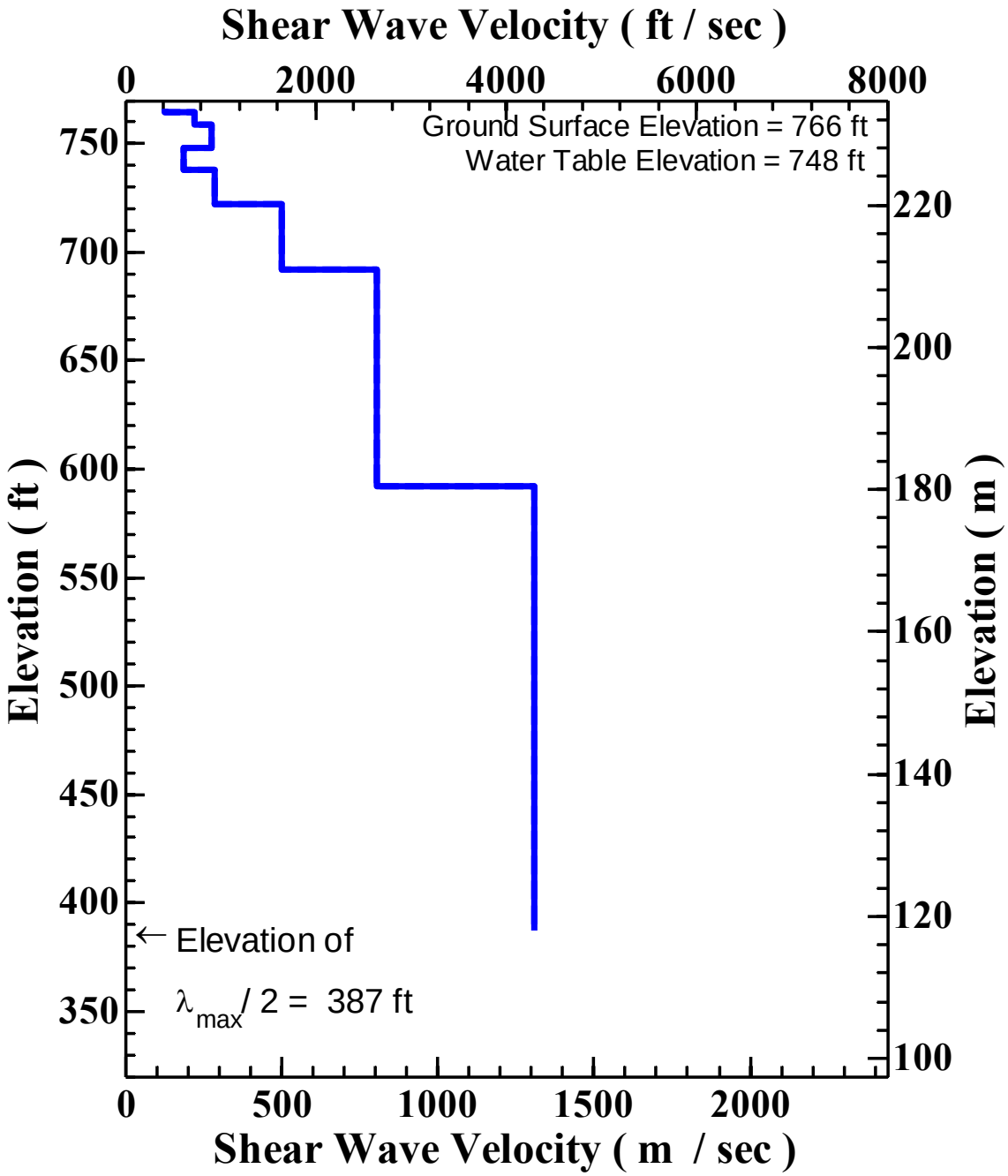

Figure B.8 Shear Wave Velocity Profile for Site 8

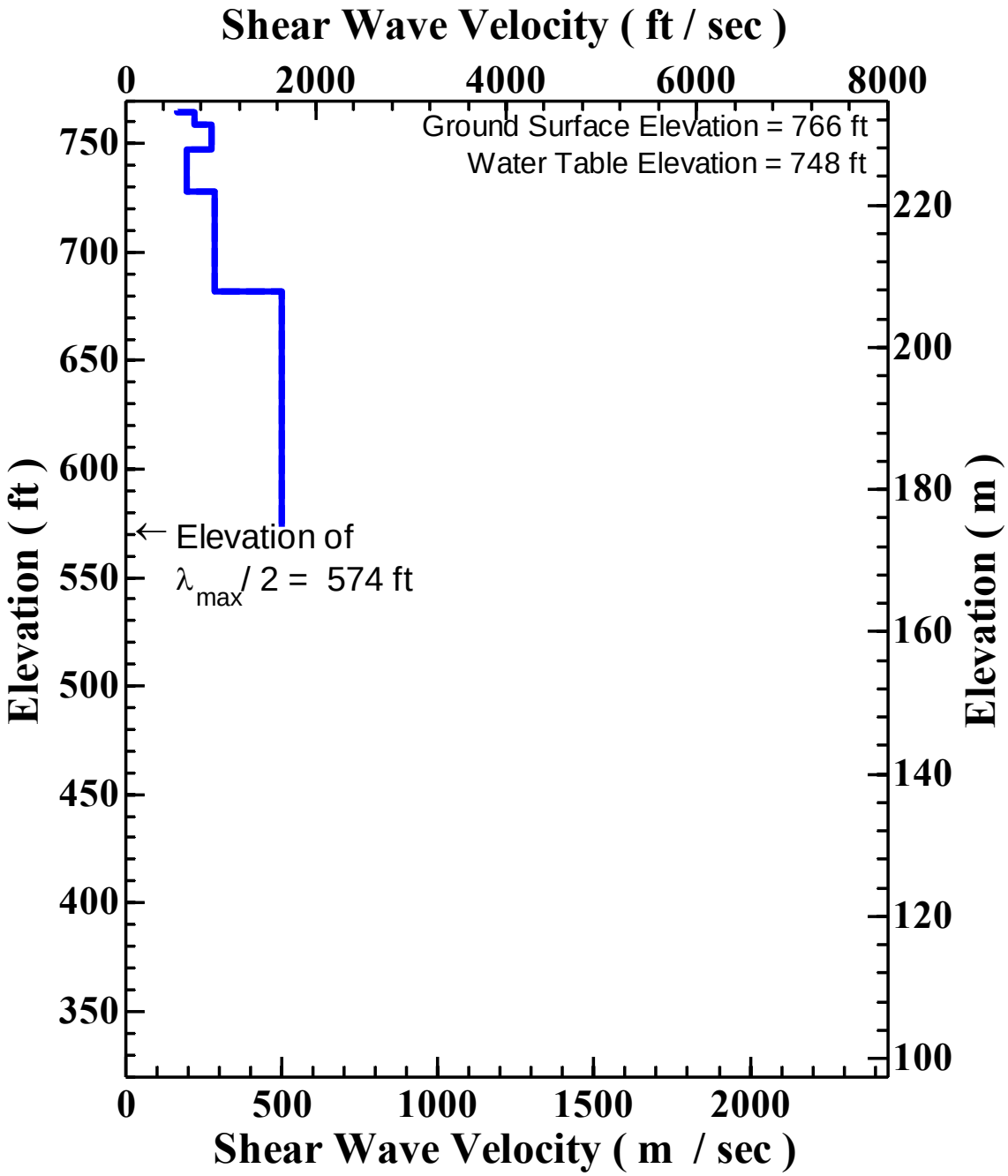

Figure B.9 Shear Wave Velocity Profile for Site 9

Appendix C

Interpreted V_s Profiles of the 9 SASW Test Sites at the Kingston Fly Ash Recovery Project, Harriman, TN

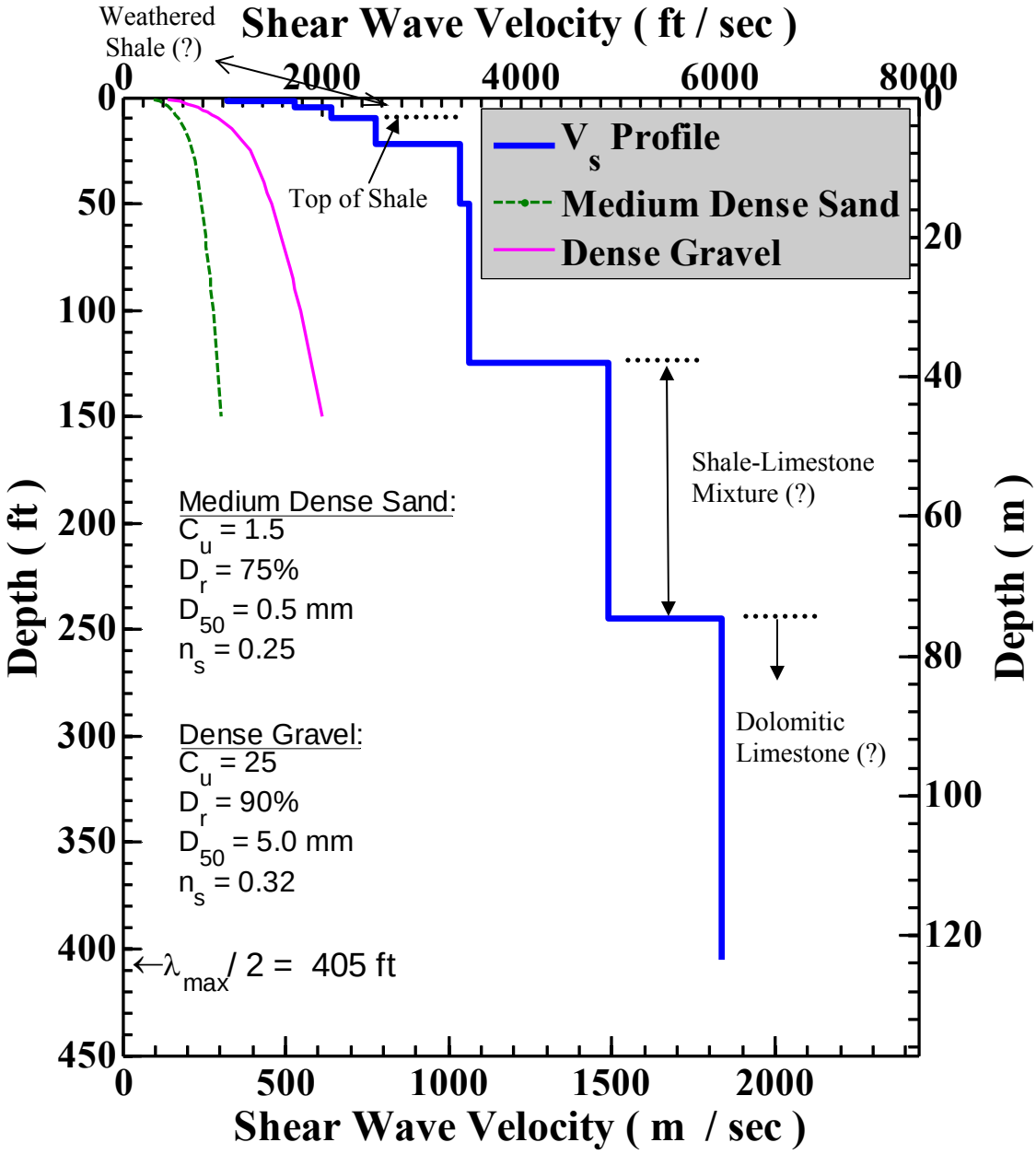

Figure C.1 Shear Wave Velocity Profile with Interpreted Geological Material Boundaries at SASW Site 1

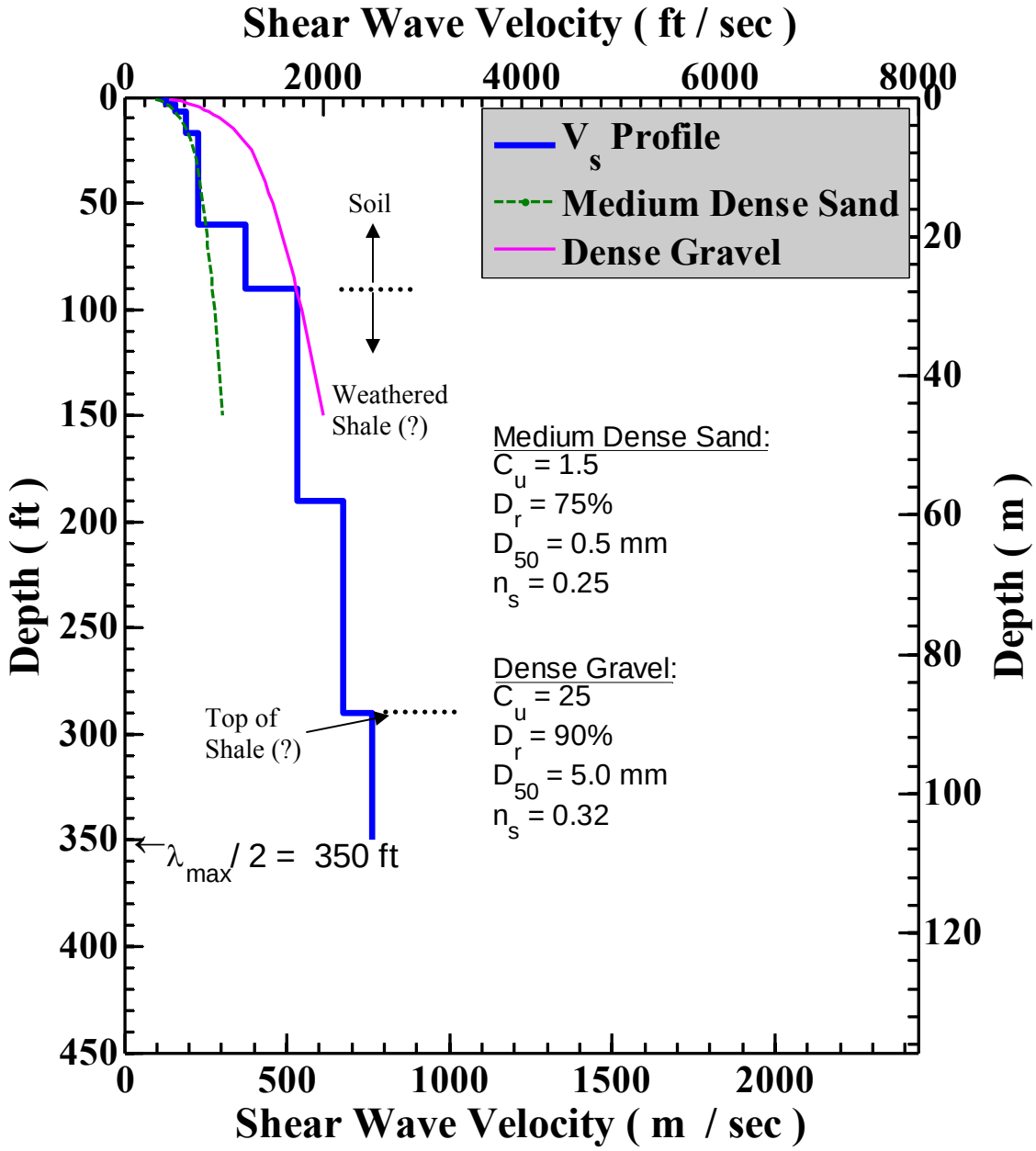

Figure C.2 Shear Wave Velocity Profile with Interpreted Geological Material Boundaries at SASW Site 2

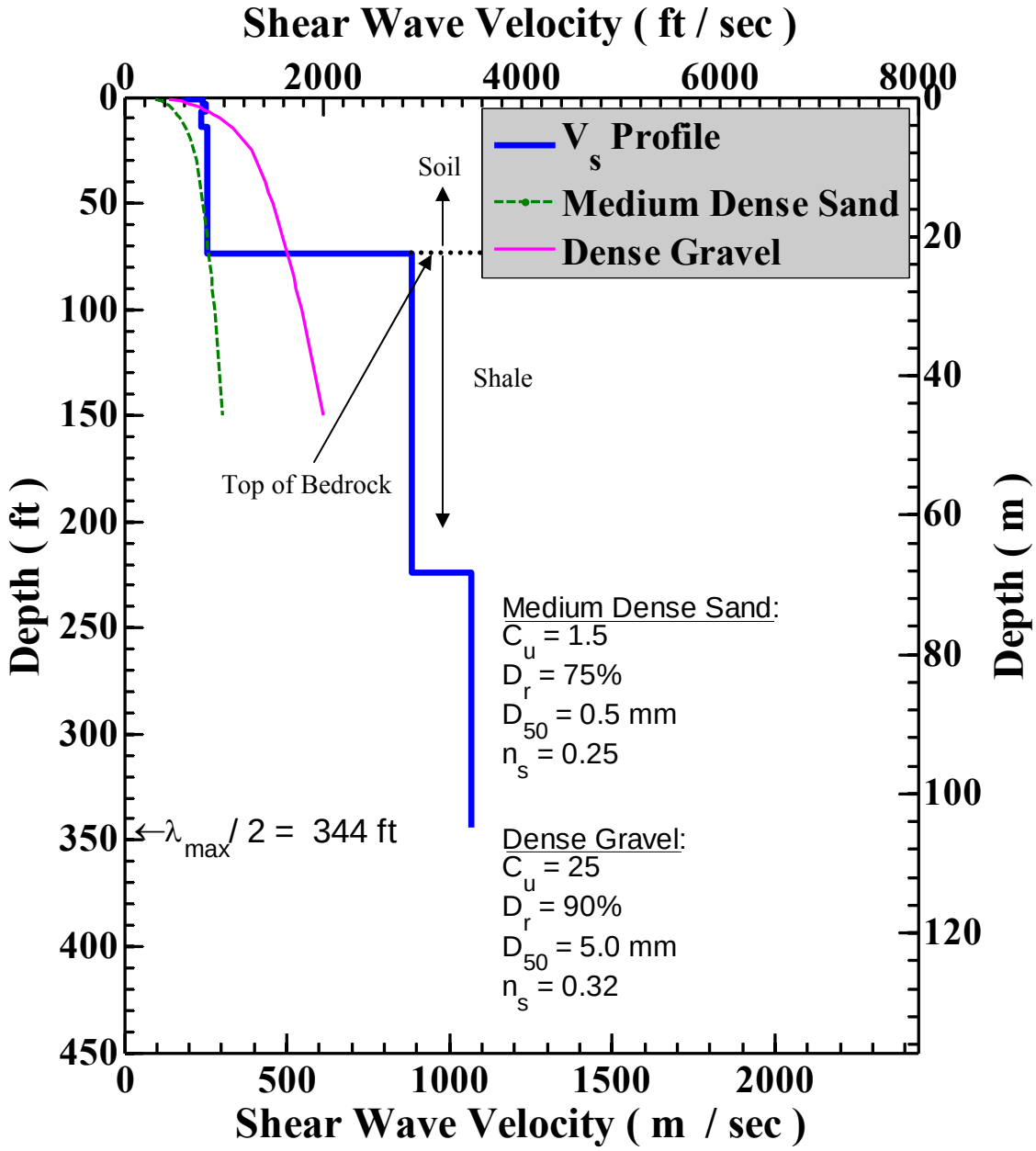

Figure C.3 Shear Wave Velocity Profile with Interpreted Geological Material Boundaries at SASW Site 3

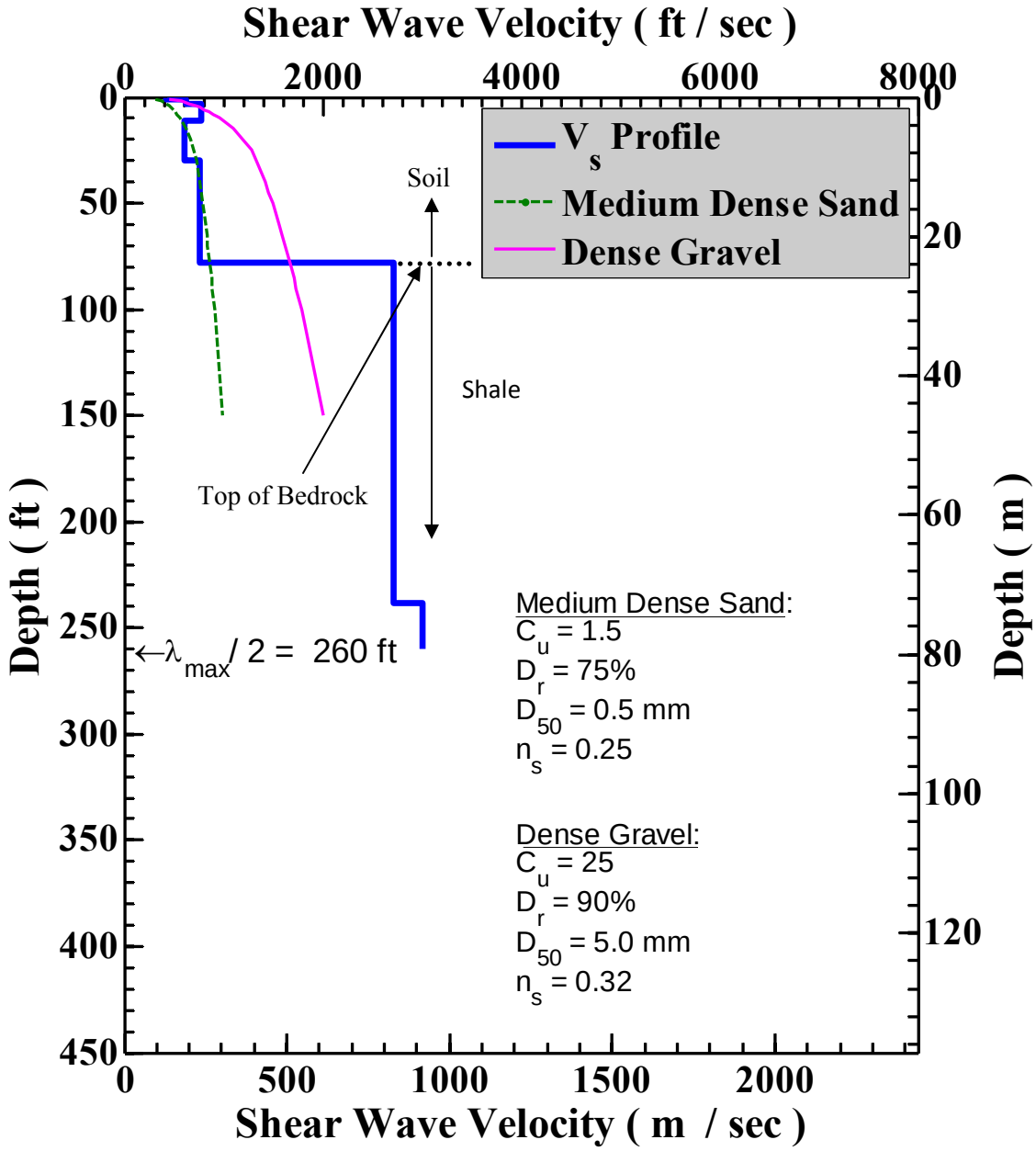

Figure C.4 Shear Wave Velocity Profile with Interpreted Geological Material Boundaries at SASW Site 4

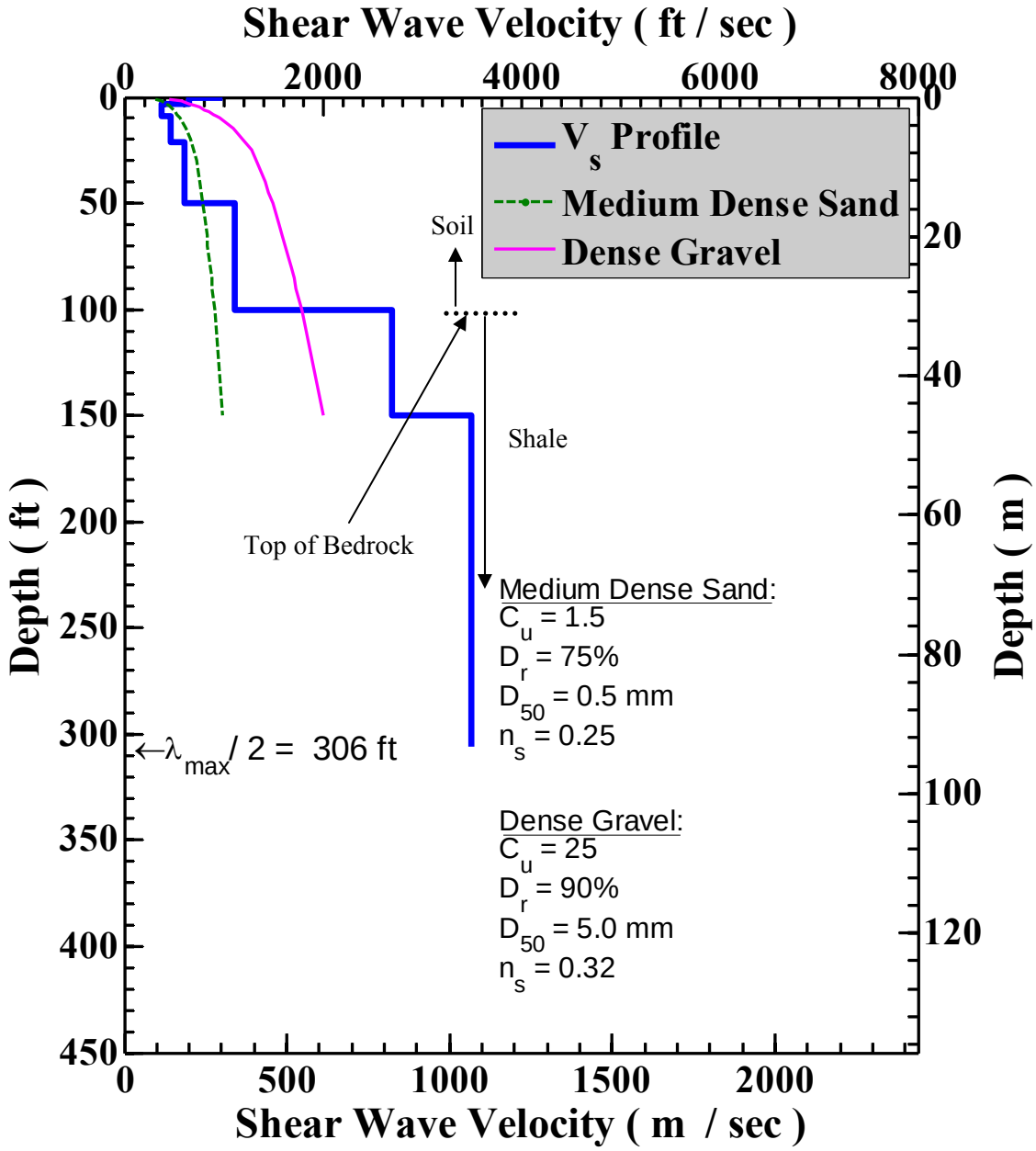

Figure C.5 Shear Wave Velocity Profile with Interpreted Geological Material Boundaries at SASW Site 5

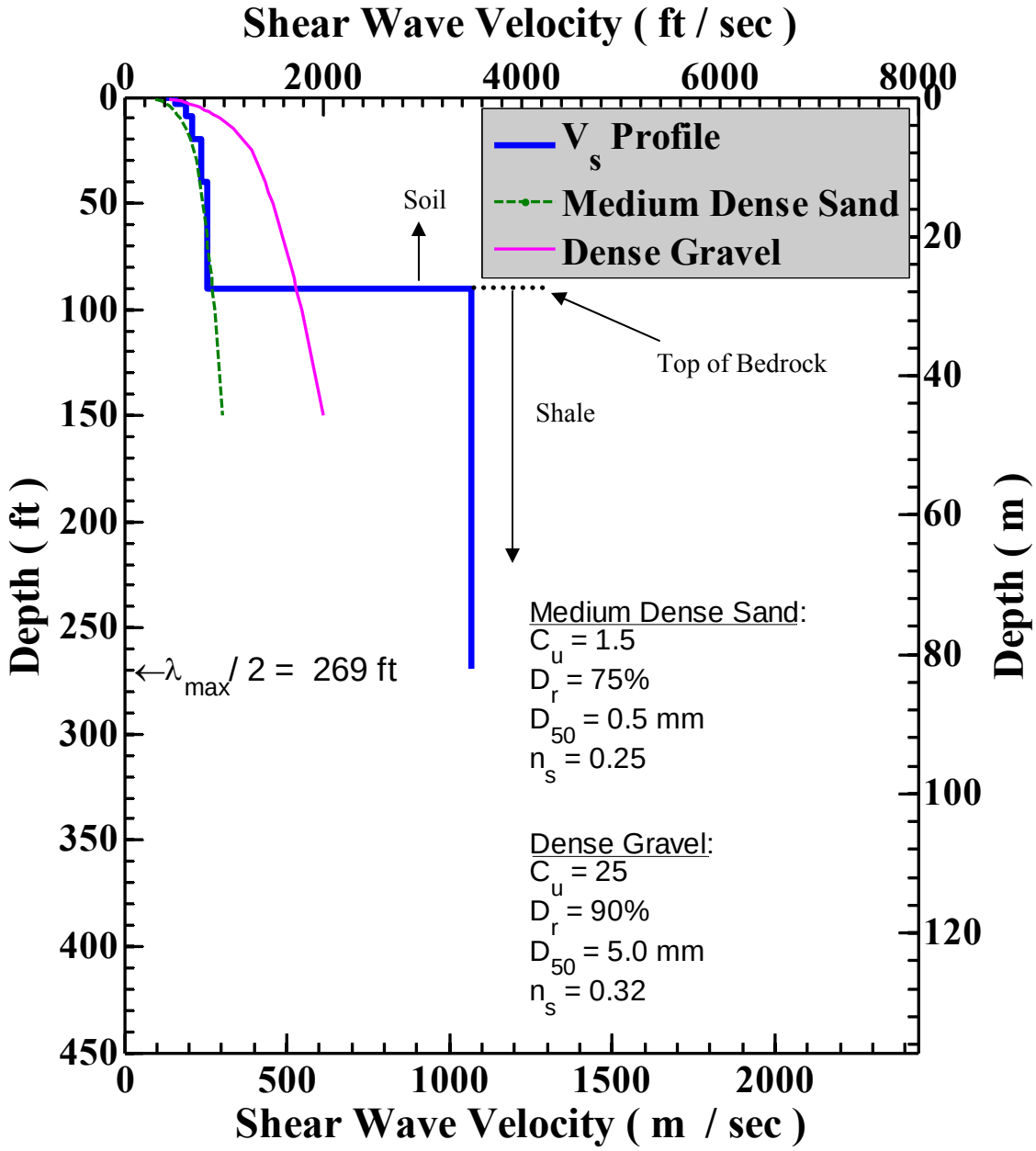

Figure C.6 Shear Wave Velocity Profile with Interpreted Geological Material Boundaries at SASW Site 6

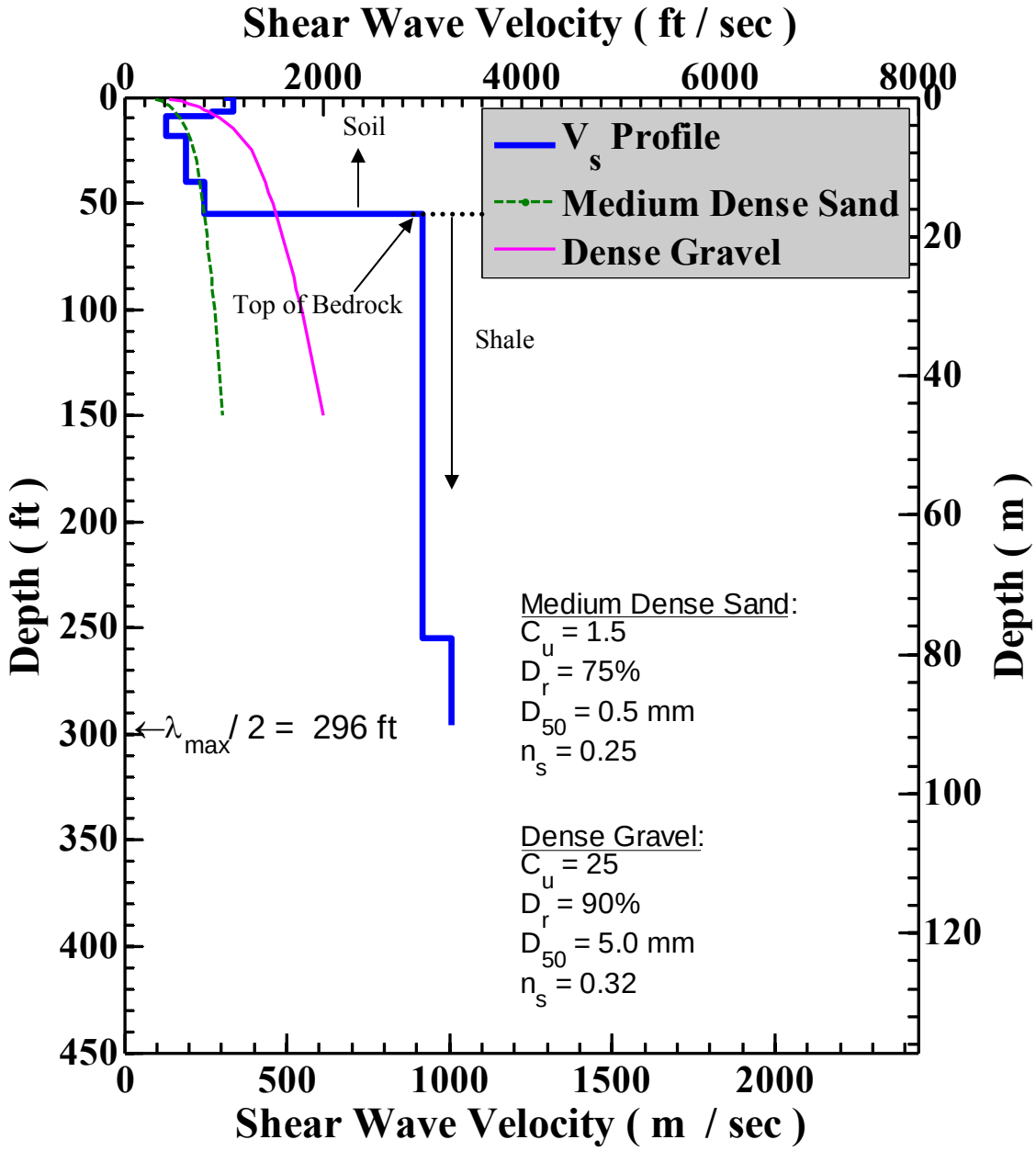

Figure C.7 Shear Wave Velocity Profile with Interpreted Geological Material Boundaries at SASW Site 7

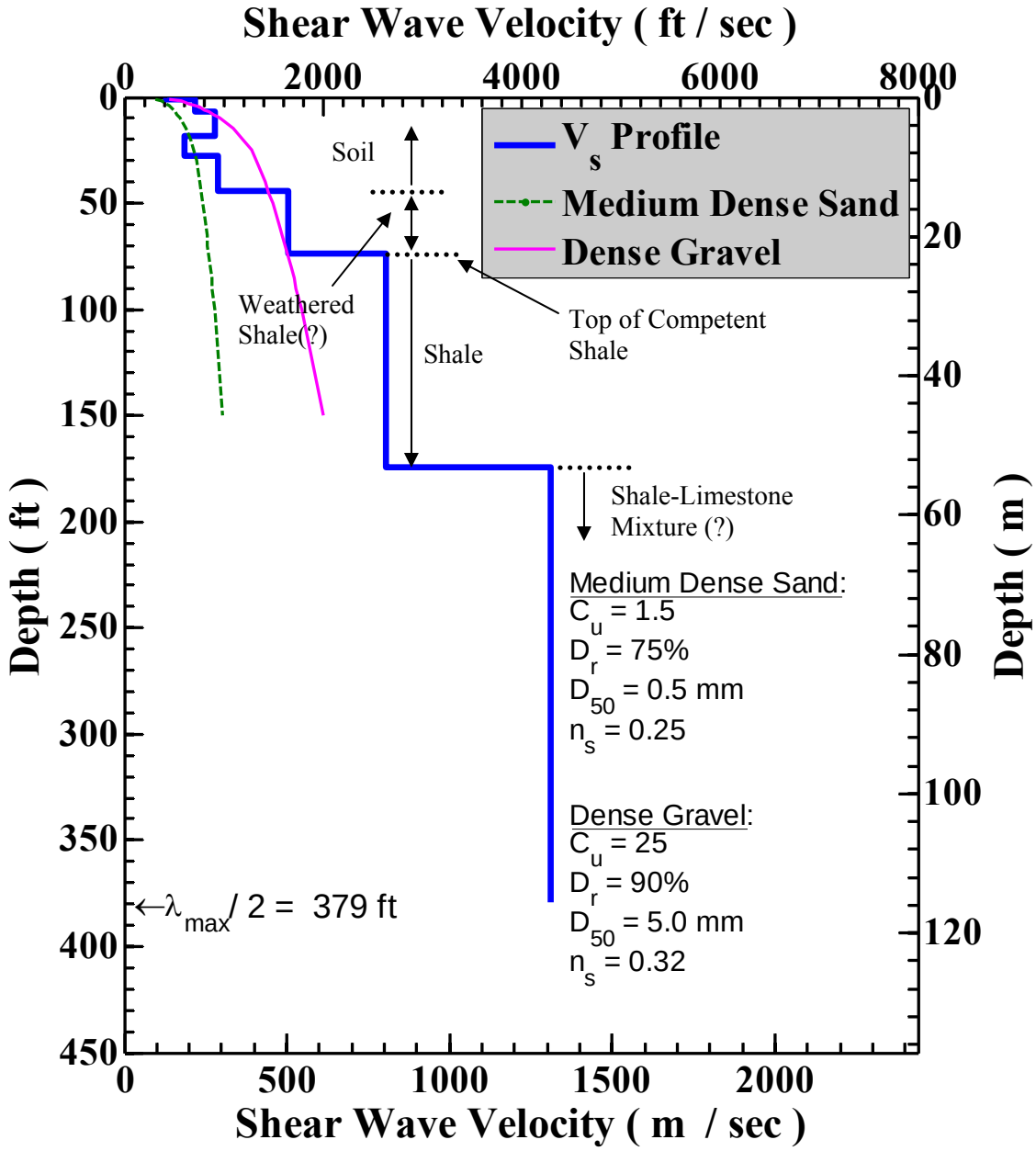

Figure C.8 Shear Wave Velocity Profile with Interpreted Geological Material Boundaries at SASW Site 8

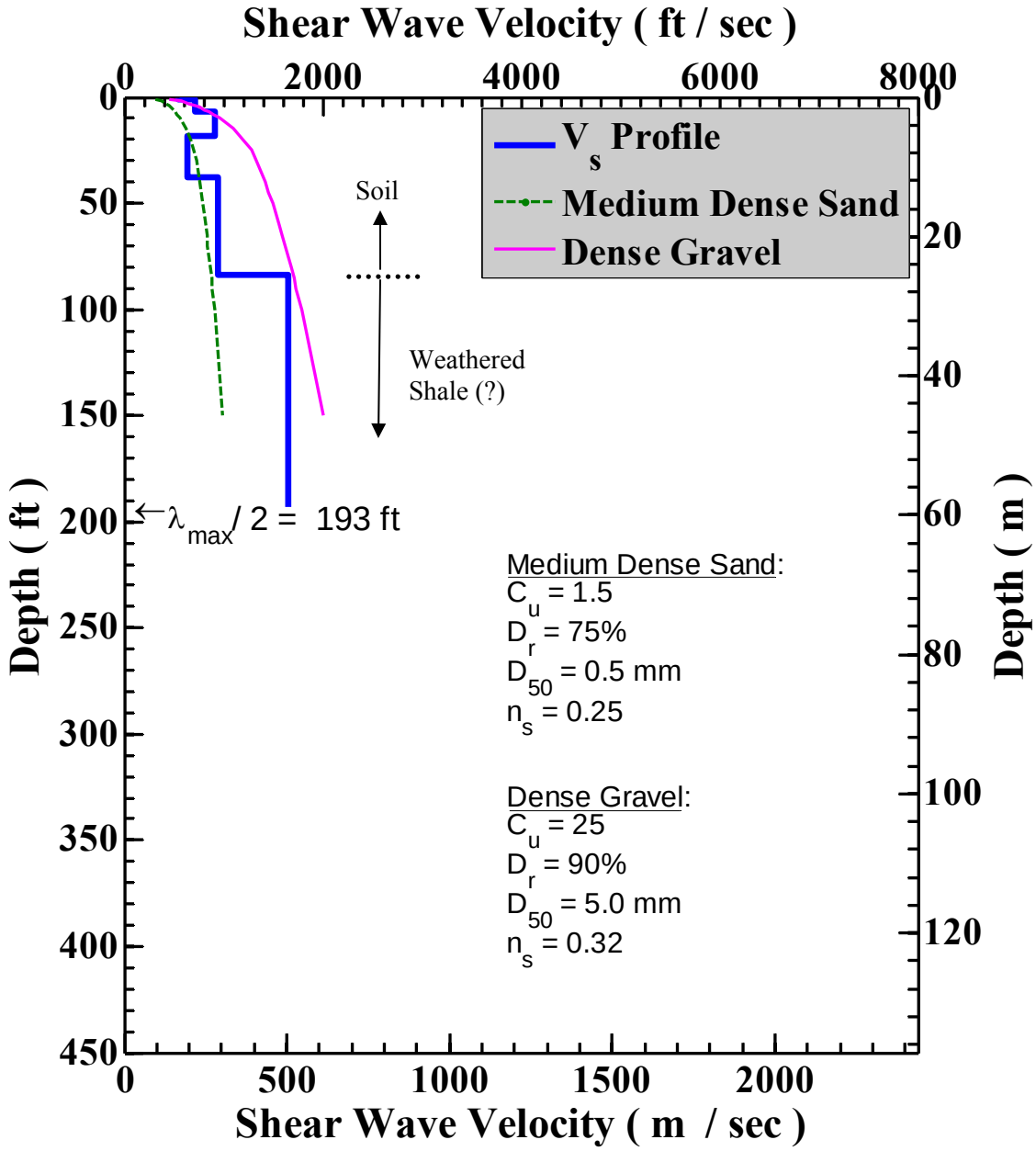

Figure C.9 Shear Wave Velocity Profile with Interpreted Geological Material Boundaries at SASW Site 9